On the Mechanism of Urea-Induced Protein Denaturation

Matteus Lindgren

Department of Chemistry
901 87 Umeå
Umeå 2010
Sweden

ISBN: 978-91-7264-997-2
Printed by: VMC KBC
Umeå, Sweden 2010

Nobody climbs mountains for scientific reasons. Science is used to raise money for the expeditions, but you really climb for the hell of it.

Edmund Hillary

Table of Contents

List of Papers

This thesis is based on the following papers, which are referred to in the text by the Roman numerals I-III. The papers can be found as reprints at the end of the thesis.

I. **M. Lindgren**, P.-O. Westlund

On the stability of Chymotrypsin Inhibitor 2 in a 10 M urea solution. The role of interaction energies for urea-induced protein denaturation.

Accepted for publication in Phys. Chem. Chem. Phys.

II. **M. Lindgren**, T. Sparrman, P.-O. Westlund

A combined molecular dynamic simulation and urea ^{14}N NMR relaxation study of the urea-lysozyme system

Spectrochimica Acta Part A, 2010, **75**, 953

III. **M. Lindgren,** P.-O. Westlund

The affect of urea on the kinetics of local unfolding processes in Chymotrypsin Inhibitor 2

Submitted to Biophysical Chemistry

Abstract

It is well known that folded proteins in water are destabilized by the addition of urea. When a protein loses its ability to perform its biological activity due to a change in its structure, it is said to *denaturate*. The mechanism by which urea denatures proteins has been thoroughly studied in the past but no proposed mechanism has yet been widely accepted. The topic of this thesis is the study of the mechanism of urea-induced protein denaturation, by means of Molecular Dynamics (MD) computer simulations and Nuclear Magnetic Resonance (NMR) spectroscopy.

Paper I takes a thermodynamic approach to the analysis of protein – urea solution MD simulations. It is shown that the protein – solvent interaction energies decrease significantly upon the addition of urea. This is the result of a decrease in the Lennard-Jones energies, which is the MD simulation equivalent to van der Waals interactions. This effect will favor the unfolded protein state due to its higher number of protein - solvent contacts. In Paper II, we show that a combination of NMR spin relaxation experiments and MD simulations can successfully be used to study urea in the protein solvation shell. The urea molecule was found to be dynamic, which indicates that no specific binding sites exist. In contrast to the thermodynamic approach in Paper I, in Paper III we utilize MD simulations to analyze the affect of urea on the kinetics of local processes in proteins. Urea is found to passively unfold proteins by decreasing the refolding rate of local parts of the protein that have unfolded by thermal fluctuations.

Based upon the results of Paper I – III and previous studies in the field, I propose a mechanism in which urea denatures proteins mainly by an enthalpic driving force due to attractive van der Waals interactions. Urea interacts favorably with all the different parts of the protein. The greater solvent accessibility of the unfolded protein is ultimately the factor that causes unfolded protein structures to be favored in concentrated urea solutions.

1. Project Description

Proteins are the machines of living organisms. They are responsible for the construction, the maintenance and the degradation of the cells constituting the organism, but they are also involved in the communication and transport of substances between the cells. Proteins are long molecular chains of covalently bonded units called amino acids. The genetic code incorporated into the DNA molecule includes information about the sequence of amino acids that are to be linked together in order to produce a specific protein. However, for the protein to be able to perform its biological function, a specific structure and the right amount of structural flexibility needs to be incorporated, in addition to the correct sequence of amino acids. The process when a protein undergoes a transition from the unstructured polymer to a compact three-dimensional structure is termed *protein folding*. The structure that the protein adopts is determined by the chemical and physical properties of its inherent amino acids in combination with the local molecular environment. As for any chemical equilibria, protein folding can be characterized by thermodynamic parameters. The change in Gibbs free energy during the folding process is termed *the stability* of the protein, since it determines whether the folded or the unfolded protein structure is the most stable. A protein that folds without intermediates is said to exhibit two-state folding and the folding equilibrium can for such a protein be written as

$$U \underset{k_u}{\overset{k_f}{\rightleftharpoons}} F \tag{1}$$

where U denotes the ensemble of unfolded proteins and F denotes the folded protein structures. k_f and k_u are the rate constants for folding and unfolding, respectively. These will determine the Gibbs standard free energy of folding, as well as the concentration of folded and unfolded protein according to equations (2) and (3).

$$\Delta G^o_{U\rightarrow F} = -RT \ln K = -RT \ln \frac{k_f}{k_u} \tag{2}$$

$$\frac{[F]}{[U]} = \frac{k_f}{k_u} \tag{3}$$

where K is the equilibrium constant and $[F]$ and $[U]$ are the concentrations of folded protein and unfolded protein, respectively. These equations tell us that the protein folding equilibrium is dynamic, *i.e.* that some proteins in the

sample will fold while others unfold at the same time. The equilibrium concentrations of the folded and the unfolded species are reached when they match the rates of conversion from one species to the other. It is therefore equally valid to consider the unfolding reaction as being the forward reaction, *i.e.* we consider the reaction

$$F \underset{k_f}{\overset{k_u}{\rightleftharpoons}} U \tag{4}$$

for which the Gibbs standard free energy can be written as:

$$\Delta G^o_{F\to U} = -RT \ln \frac{k_u}{k_f} = -\Delta G^o_{U\to F} \tag{5}$$

A protein that exhibits two-state folding and unfolding has a relatively smooth free energy landscape with only two dominating minima along the folding pathway. The free energy barrier that separates the two minima corresponds to a transition state (TS) protein structure. Transition state theory allows us to connect the relative height of the barrier versus the two minima, ΔG^o_{F-TS} and ΔG^o_{U-TS}, with the rate constants k_u and k_f:

$$k_u = \kappa \frac{k_B T}{h} \exp\left(\frac{-\Delta G^o_{F-TS}}{RT}\right) \tag{6}$$

$$k_f = \kappa \frac{k_B T}{h} \exp\left(\frac{-\Delta G^o_{U-TS}}{RT}\right) \tag{7}$$

where κ, k_B and h is the transmission coefficient, Boltzmann´s constant and Planck´s constant, respectively[1]. A schematic free energy landscape of a protein that exhibits two-state folding is displayed in Fig. 1.

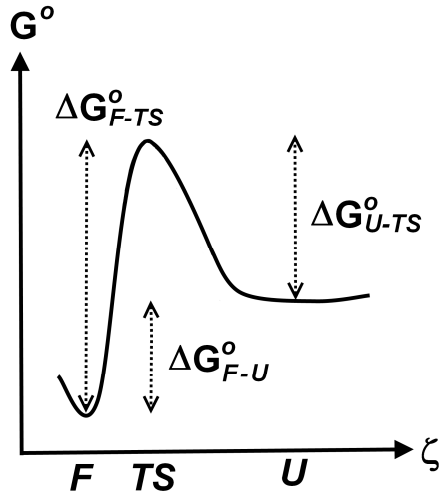

Fig. 1. Schematic free energy landscape of a protein in water that exhibits two-state folding. The reaction coordinate ζ represents the averaged folding / unfolding pathway.

The equilibrium between the folded and the unfolded protein structures will be governed by the interplay between protein – protein interactions, solvent – solvent interactions and protein – solvent interactions. Folding of a protein increases the number of protein – protein contacts and solvent – solvent contacts. Unfolding on the other hand increases the solvent accessible surface area of the protein and therefore the number of protein – solvent contacts. If the interactions between the protein and the solvent are more favorable (in a general sense), the dominating protein structure will be the unfolded form, rather than the folded form. The stability of a folded protein depends upon several factors, such as the type of solvent, the pH, the ionic strength and the temperature. It has been known for a century that the addition of urea, $H_2N\text{-}CO\text{-}NH_2$, to a protein – water solution destabilizes the folded protein structure[2]. The unfolded protein structures dominate at high urea concentrations for all but the most stable proteins. When a protein loses its ability to perform its biological activity due to a change in its structure, it is said to *denaturate*. Urea is therefore called a *denaturant*. Urea is by no means the only substance that can destabilize proteins[3]. Another well-known denaturant is the salt guanidinium chloride. Other molecules, such as trimethylamine N-oxide (TMAO), have a large stabilizing effect on proteins. The research field of *chemical denaturation* incorporates all denaturants and their effect on proteins.

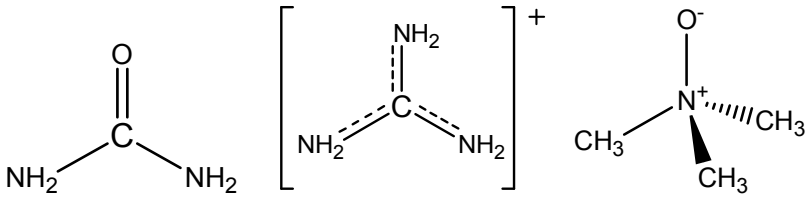

Urea Guanidinium ion TMAO

When urea is added, the unfolding free energy decreases, from a positive value to a negative value at high concentrations. Stopped flow studies, see for example Ref. 4, have shown that the unfolding free energy is decreased in urea solutions by means of an increased unfolding rate while the folding rate decreases by approximately the same amount, but the exact behavior depends upon the type of protein. This means that ΔG^{o}_{F-TS} is decreased and ΔG^{o}_{U-TS} is increased in the presence of urea. The change of the unfolding free energy landscape due to urea is schematically shown in Fig. 2.

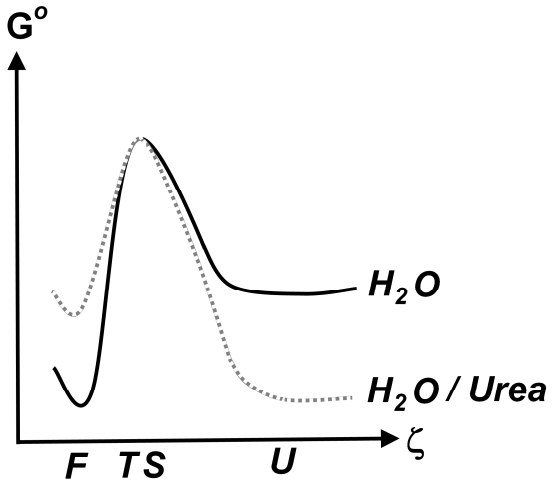

Fig. 2. Schematic free energy landscape that shows the affect of urea on the relative barrier heights of a protein. Note that the absolute height of the barrier may also be changed by urea but it is assumed to be unchanged in this figure.

Motivation for the project

Urea has a very widespread use in laboratory experiments due to its ability to unfold proteins without reacting with the proteins. Urea is for example used in protein folding research as well as in studies concerning the effect of mutations on the protein properties. The extensive use of urea in research creates a need to understand the mechanism by which urea destabilizes proteins. Urea solutions have also gained attention due to the general importance of understanding how the interactions between a protein and its chemical environment affect the structure and the dynamics of the protein. The research field of chemical denaturation has therefore been extensively studied both in the past and at present. However, the mechanism of urea-induced denaturation is still not known in detail.

Aim of the project

The aim was to study the effects of urea on water and on proteins in order to retrieve information regarding urea-induced denaturation.

2. Methods

2.1. Molecular Dynamics Simulations

The first scientific work utilizing Molecular Dynamics (MD) computer simulations was published in 1957[5]. Even though five decades have passed, their description of the method of MD simulations still applies: "The method consists of solving exactly (to the number of significant figures carried) the simultaneous classical equations of motion of several hundred particles by means of fast electronic computors." However, due to the dramatically increased computer performance during the years that have since passed, the scale of the systems that are possible to study has now increased from several hundred particles and 200 000 collisions to 100 000 atoms and micro seconds of simulation time. MD simulations are now routinely used in research involving molecular systems[6]. Not only the hardware but also the software has evolved. A number of sophisticated MD simulation software suites are now available. Arguably, the programs most commonly used in research of biomolecules are CHARMM[7], AMBER[8], GROMACS[9], ENCAD[10] and NAMD[11].

MD simulations are based upon classical mechanics, in contrast to simulations utilizing a varying degree of quantum mechanical theories. The advantage is the lower computational cost and therefore the ability to study phenomena taking place on a longer time scale and/or larger systems. The disadvantage is that electrons cannot be explicitly treated. This limits MD simulations to studies without chemical reactions. In addition, the accuracy of the simulations depends on how well the quantum mechanical energy landscape can be approximated by an effective potential, governed by the laws of classical physics. For a system consisting of N particles, the core of the MD simulation algorithm consists of solving Newton´s equation of motion for an N particle system:

$$m\frac{d^2\boldsymbol{r}_i}{dt^2} = \boldsymbol{F}_i, i = 1 \dots N \tag{8}$$

The forces $\boldsymbol{F}_i$ are the gradient of the potential energy $U(\boldsymbol{r}_1, \boldsymbol{r}_2, \dots \boldsymbol{r}_N)$

$$\boldsymbol{F}_i = -\frac{\partial U(\boldsymbol{r}_i)}{\partial \boldsymbol{r}_i} \tag{9}$$

When the force acting on each particle has been acquired at a specific time t, numerical integration of the equations of motion yields new particle positions at a time $(t + \Delta t)$. However, several algorithms are available for the

integration. Based on a Taylor expansion of the positions at time *t*, the Euler algorithm in Eq. (10) seems to be the natural choice.

$$\boldsymbol{r}_i(t+\Delta t) = \boldsymbol{r}_i(t) + \boldsymbol{v}_i(t)\Delta t + \frac{\boldsymbol{F}_i(t)}{2m_i}(\Delta t)^2 \tag{10}$$

where $\boldsymbol{v}_i$ is the velocity of particle *i*. Unfortunately, the Euler algorithm has some inherent problems. For example, it is not time reversible and it also suffers from a large energy drift. It is therefore common to use other algorithms, such as the Verlet algorithm, the velocity Verlet algorithm or the Leap-Frog algorithm. The Leap-Frog algorithm constitutes Eq. (11) and (12) [12].

$$\boldsymbol{r}_i(t+\Delta t) = \boldsymbol{r}_i(t) + \boldsymbol{v_i}\left(t+\frac{\Delta t}{2}\right)\Delta t \tag{11}$$

$$\boldsymbol{v_i}\left(t+\frac{\Delta t}{2}\right) = \boldsymbol{v_i}\left(t-\frac{\Delta t}{2}\right) + \frac{\boldsymbol{F_i}}{m_i}\Delta t \tag{12}$$

MD simulations commonly utilize pair-potentials, *i.e.* the potential energy and the force of each particle in the system is calculated by a sum of two-particle interactions. In order to calculate the potential energy for a given set of particle coordinates, one must first define the set of equations describing the different interactions that occur in the system, *i.e.* the *force field* must be defined. The most common type of force field utilized in MD simulations of biomolecules is the Class I type. The terms included in this force field are common among the most widely used MD simulation programs such as CHARMM, AMBER and GROMACS. An example of a Class I potential energy function is displayed in Eq. (13) - (15).

$$U = U_{bonded} + U_{non-bonded} \tag{13}$$

$$\begin{aligned} U_{bonded} = & \sum_{bonds} K_b(r-r_0)^2 \\ & + \sum_{angles} K_\theta(\theta-\theta_0)^2 \\ & + \sum_{dihedrals} K_\chi(1+\cos(n\phi-\delta)) \\ & + \sum_{impropers} K_{imp}(\psi-\psi_0)^2 \end{aligned} \tag{14}$$

$$U_{non-bonded} = \frac{1}{2}\sum_i \sum_{j \neq i} \left\{ 4\varepsilon_{ij} \left[\left(\frac{\sigma_{ij}}{r_{ij}} \right)^{12} - \left(\frac{\sigma_{ij}}{r_{ij}} \right)^{6} \right] + \frac{q_i q_j}{4\pi\varepsilon r_{ij}} \right\} \qquad (15)$$

The function that treats bonded interactions between atoms, Eq. (14), is composed of terms that represent bond vibration (2 atoms), angle vibration (3 atoms) and movement around torsion angles, *i.e.* the dihedrals and the impropers (4 atoms), see Fig. 3.

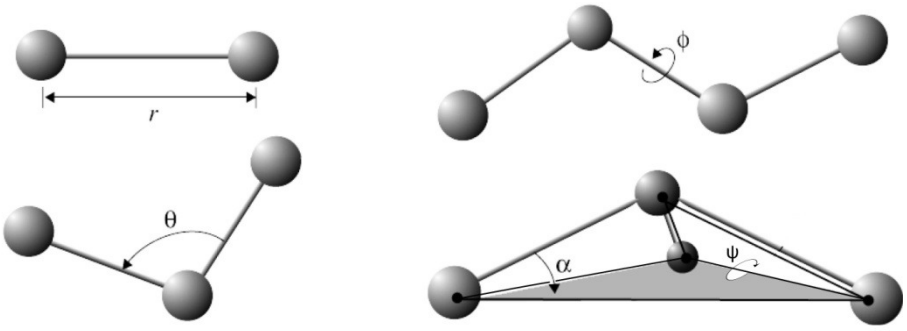

Fig. 3. Coordinates for bonded interactions[13].

The non-bonded potential, Eq. (15), consists of the Lennard-Jones potential followed by the electrostatic potential. The r_{ij}^{-12} - term in the Lennard-Jones potential represents repulsion due to overlap of the electron orbitals originating from different atoms. Since explicit electrons and polarizability are excluded from classical MD simulations, the dispersion and the Debye interactions are treated by the r_{ij}^{-6}-term of the Lennard-Jones potential. Hydrogen bonds are not treated separately but *via* a combination of the Lennard-Jones potential and the electrostatic potential.

Differences among the force fields used in MD simulation software are commonly not in the form of the used potential energy function, but rather in the parameters of the force field. These are optimized by fitting the potential energy function, and functions derived from it, to target data in the form of experimental data or quantum mechanical data of model compounds. The choice of target data is important. The simplicity of the potential energy function (as compared to its quantum mechanical counterpart) will inevitably create deviations in the physical properties that the force field has not been optimized for. This should be remembered when choosing a force field for a project. Target data extracted from quantum mechanical calculations are appealing since a number of properties can be

readily calculated from all molecules of small size. However, a drawback with quantum mechanical data is the difficulties in treating molecules in the condensed phase. Since the properties of molecules in the gas phase are significantly altered when put in a surrounding liquid, there is still a need for experimental data in the parameter optimization[14].

MD simulations in different ensembles

A molecular system can be viewed on different levels. On the microscopic level, all molecular details are accessible to the observer but on the macroscopic level, only system-wide and average properties of the system are accessible. The statistical mechanical construct of an *ensemble* is the collection of all the microscopic states that are consistent with a certain macroscopic state. For example, the *microcanonical ensemble* of a system is the collection of all microscopic states of that system that are consistent with a fixed number of particles N, a fixed system volume V and a fixed total energy E, in short (N,V,E). The *canonical ensemble* has a fixed temperature instead of energy, *i.e.* it is characterized by (N,V,T). The *isobaric-isothermal ensemble* is characterized by (N,p,T). Other ensembles can also be constructed. The difference between ensembles becomes negligible for large systems[20].

Arguably, the most straightforward MD simulation algorithm produces simulations belonging to the microcanonical ensemble. However, other algorithms that extend MD simulations to incorporate other ensembles have been constructed. The thermostat algorithm by Andersen[15] can be used to produce simulations of the canonical ensemble by coupling the simulation system to an external heat bath. Stochastic collisions with virtual particles make sure that the simulated particles have velocities that belong to a Maxwell-Boltzmann distribution of the desired temperature. However, caution should be taken as the stochastic collisions can affect dynamic properties of the system[12]. Simulations with a constrained temperature and / or pressure can be realized by making use of the algorithms of Berendsen et al.[16]. The system is then weakly coupled to an external heat bath or pressure bath by scaling the particles´ velocities. Unfortunately, this method does not yield correct ensembles since the fluctuations of the kinetic energy of the system are reduced. This can be problematic for small systems and large coupling factors but the deviations from the proper ensembles are in general very small[26]. Strictly correct simulations in the isobaric-isothermal ensemble can instead be performed by utilizing the extended system approach as in the thermostat of Nosé-Hoover[17,18] and the barostat of Parrinello-Rahman[19].

Performing experiments in MD simulations

As far as we know, nature is governed by the laws of quantum mechanics. Since experiments are performed on (a part of) nature, these experiments are performed on quantum mechanical systems. The algorithms of MD simulations are based upon classical mechanics and when a computer experiment is performed inside an MD simulation, the experiment is performed on a system governed by the laws of classical mechanics. It is not obvious therefore, that the results from experiments performed in MD simulations should be in agreement with the results of practical experiments. When we perform a large number (an infinite number) of measurements of a certain observable A on a quantum mechanical system, the average value of A thus obtained is the ensemble average. For a system in the canonical ensemble, the ensemble average of A is calculated as

$$\langle A \rangle = \frac{\sum_i \exp\left(-E_i / k_B T\right) \langle i|A|i \rangle}{\sum_i \exp\left(-E_i / k_B T\right)} \tag{16}$$

where the summations over i correspond to summations over all energy eigenstates $|i\rangle$ of the system and E_i is the corresponding eigenvalue of the total system energy. For systems in the classical limit, *i.e.* systems with low particle density and / or high temperature, it can be shown[12,20] that the quantum mechanical ensemble average of Eq. (16) has a classical analogue given by

$$\langle A \rangle = \frac{\int d\boldsymbol{p}^N d\boldsymbol{r}^N \exp\left[-\frac{E(\boldsymbol{p}^N, \boldsymbol{r}^N)}{k_B T}\right] A(\boldsymbol{p}^N, \boldsymbol{r}^N)}{\int d\boldsymbol{p}^N d\boldsymbol{r}^N \exp\left[-\frac{E(\boldsymbol{p}^N, \boldsymbol{r}^N)}{k_B T}\right]} \tag{17}$$

where $\boldsymbol{p}$ and $\boldsymbol{r}$ are the momentum vector and the position vector of a particle, respectively. When comparing Eq. (16) with Eq. (17), we see that the summation over states in Eq. (16) is replaced by integration over phase space when the system is treated classically. Simulations of biomolecules are typically performed close to physiological conditions, which permits the use of Eq. (17) for the analysis of these systems. In practice, calculations of ensemble averages by using Eq. (17) are only possible for very small systems, since they require evaluation of two 6N dimensional integrals and quickly becomes very computationally demanding when the number of particles N increases. Instead, a representative part of phase space is sampled by an MD simulation over a finite amount of time and the ensemble average of A in Eq. (17) is replaced by the time average of A as sampled from the simulation. This methodology is validated by the *ergodic hypothesis*, which states that

time averages are equal to ensemble averages in the limit of infinite sampling time[20].

The primary result of MD simulations is the evolution in time of the momentum and the coordinates of all particles. In order to evaluate $A(\boldsymbol{p}^N, \boldsymbol{r}^N)$ in Eq. (17), one must first express the observable as a function of the momentum and the coordinates. For example, the pressure of a system in the canonical ensemble can be calculated as[12]

$$p = \rho k_B T + \frac{1}{3V}\left[\sum_{i<j} -\frac{\partial U(\boldsymbol{r}_{ij})}{\partial \boldsymbol{r}_{ij}} \cdot \boldsymbol{r}_{ij}\right] \tag{18}$$

MD simulations are dynamic, *i.e.* the evolution in time of the system is simulated, and dynamic properties can therefore be calculated. This is in contrast to Monte Carlo simulations where the ensemble average of Eq. (17) is evaluated statically. The calculation of the self-diffusion coefficient can be taken as an example of a dynamic property. It can be calculated from the Einstein relation[12]

$$D = \frac{1}{2d} \cdot \left(\frac{d\langle \Delta r^2(t)\rangle}{dt}\right) \tag{19}$$

where d is the dimensionality of the system and

$$\langle \Delta r^2(t)\rangle = \frac{1}{N}\sum_{i=1}^{N} |\Delta \boldsymbol{r}_i(t)|^2 \tag{20}$$

It can be mentioned that transport coefficients, such as the diffusion coefficient, can also be calculated by utilizing the results of linear response theory[12,20,21,22]. The Green-Kubo relations connect transport coefficients with integrals over time-correlation functions. The diffusion coefficient of a particle in a three-dimensional system is related to the velocity time-correlation function according to Eq. (21).

$$D = \frac{1}{3}\int_0^\infty \langle \boldsymbol{v}(t) \cdot \boldsymbol{v}(t+\tau)\rangle \, d\tau \tag{21}$$

Accelerating MD simulations

The choice of the computer simulation method and the setup of the simulation are often based upon the balance of accuracy versus speed. A high simulation speed opens up the possibility to study a larger system or, alternatively, the same system for a longer time. In order to extract a certain property of the system with a good statistical accuracy, a long simulation time is needed as compared to the correlation time of the corresponding property. In this respect, speed and accuracy is the same thing in a computer simulation. A number of tricks that are utilized in MD simulations in order to tackle the ever-present problem of inadequate speed are presented in this section.

a) The treatment of non-bonded interactions

The calculation requirement of the non-bonded interactions by using Eq. (15) is on the order of N^2 computations, where N is the number of particles in the system. It becomes very computationally expensive as the system grows and more efficient treatments of the non-bonded interactions are therefore needed. The simplest method is to truncate the energy function at some cutoff distance r_c, thereby neglecting the energy at the tail of the function, *i.e.* the contribution from distances $r > r_c$. The van der Waals potential decays quickly with distance, $U_{vdw} \propto r^{-6}$, and the Lennard-Jones term of Eq. (15), which treats the van der Waals interactions, can therefore be truncated by some cutoff method without introducing large errors.

The treatment of the electrostatic potential is more difficult, since it decays slowly with distance, $U_{Elec} \propto r^{-1}$. The use of cutoffs for the electrostatic potential is therefore not common in simulations of biomolecules, since the cutoff distance would need to be very long and many pair interactions would have to be calculated. The most common method to treat the electrostatic potential is instead the Particle Mesh Ewald (PME) method[23,24]. The basis of the Ewald techniques is to replace the slowly converging sum of electrostatic interactions between point charges by two quickly converging sums, one sum in direct space and one sum in Fourier space. In order to do so, the point charges of the original sum are screened by the addition of virtual charge distributions that are placed around the particle. The charge distributions are chosen with a total charge exactly matching the point charge of the particle but with the opposite sign. When the particle is viewed from a distance, it will seem to have a charge of zero, due to the screening of the surrounding charge distribution. The electrostatic potential will therefore quickly decay with distance. The direct space sum (or short range sum) is the sum of the electrostatic potential in the vicinity of a particle. In contrast to the sum of pure point charges, it can be truncated at short distances due to its rapid decay. However, this direct space sum includes the contribution

from the charge distributions. In order to correct for this, another set of charge distributions is added. This set is similar to the original set, but with the opposite signs on the charges. Since these charge distributions are smooth when the point charges already have been taken into account, they represent suitable data for a Fourier transform. The Fourier space sum (long range sum, reciproca space sum) is a sum over the wave vectors produced by the Fourier transform of the inverted charge distributions. Since the vectors in Fourier space represent frequencies of charge density variations rather than individual point charges, long-range electrostatic interactions are taken into account by the Fourier space sum. Only a few wave vectors need to be included in the sum since the individual charge distributions are smooth. The charge landscape is therefore sufficiently well described by a superposition of only a few waves of different frequencies. The electrostatic potential at the position of a particle can then be acquired by adding the direct space sum to the Fourier space sum after it has been subjected to an inverse Fourier transformation.

The calculation of the Fourier space sum is accelerated in the PME method by assigning the particles to a grid by using spline interpolation. Fast Fourier Transform algorithms can then be used instead of the slower traditional Fourier transforms[12,26]. The PME method is therefore significantly faster than the original Ewald summation method for all but the smallest systems. Using PME is also more accurate than using cutoffs for the same computational cost[12,26]. However, the Fast Multipole Method (FMM)[12,25] is an alternative for very large systems ($N \approx 10^5$).

b) Periodic Boundary Conditions

Even if the sample volume is only a few microliters, experiments in chemistry can (almost) always be considered as performed on a macroscopic system. This has the implication that the vast majority of the molecules probed in the experiment reside in the bulk phase, instead of in the boundary interface region. Therefore, the molecular properties probed in the experiment represent bulk phase molecules. MD simulations use *Periodic Boundary Conditions (PBC)* in order to allow a microscopic system to resemble a macroscopic system. When PBCs are activated for a simulation, the original simulation box is copied into mirror images that are placed all around the original box, see Fig. 4.

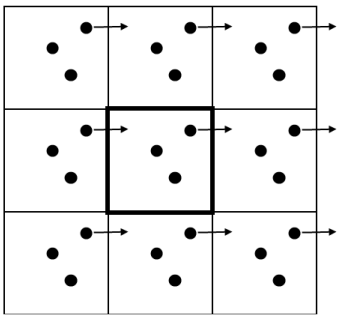

Fig. 4. Illustration of periodic boundary conditions.

The molecules on the edge of the simulation box are allowed to interact with the molecules in the mirror images. In addition, when a molecule moves outside the box, it is immediately replaced by an identical molecule, entering the box from the opposite direction. Therefore, the small microscopic simulation box resembles a macroscopic system, without any molecules at the border to vacuum or near a surface. This trick allows the simulation box to be kept small while retaining a resemblance of the molecular properties to those of a large system. However, a microscopic system that is simulated by using PBCs is still not a correct macroscopic system due to the introduced artificial periodicity. It is known that small systems with a large amount of spatial correlation may have an increased internal spatial correlation due to the use of PBCs. In such cases, the size of the simulation box should be increased and a switch to a different treatment of the electrostatic interactions should be considered[26].

c) The choice of time step

The length of the time step Δt used in the MD simulation algorithm, Eq. (11) and (12), is naturally important for the amount of simulation time one can acquire for a certain amount of computer cycles. The time step is also important since the dynamic process one wishes to study must occur on a longer time scale than the length of the time step, in order for the event to be properly sampled. In addition, the processes that do occur on long time scales will be influenced by processes that occur on much shorter time scales. A time step that is too long may not only cause unphysical behavior but may also cause the simulation to be unstable. The fastest dynamic process in simulations of biomolecules is the vibration of covalent bonds that includes hydrogen, with an oscillation time of $\approx$ 10 fs[27]. If that process is to be included in the simulation, the time step should not be longer than 1 fs. However, it is very common to assume that the vibration of hydrogen does

not influence the much larger scale processes under study, such as protein folding and unfolding. The covalent bonds that include hydrogen in both the solvent and the protein can therefore be constrained at a fixed distance by algorithms such as SHAKE[28] or LINCS[29]. The SETTLE algorithm[30] can be used for completely rigid water, *i.e.* when the bond angle of water is constrained as well as the bond lengths. Constraining covalent bonds to hydrogen allows for an increase of the time step to 2 fs. Other tricks to increase the time step exist. For example, increasing the mass of the hydrogen atom while at the same time decreasing the mass of the covalently bonded heavy atom, will decrease the oscillation frequency of that bond or angle. This allows for a longer time step. The potential functions used in the force field can also be smoothed in order to decrease the forces and thereby the dynamics of the system. Naturally, the effect of such changes must be carefully evaluated[27].

d) All-atom force fields versus United-atom force fields

The computational demand of an MD simulation algorithm scales with the number of atoms. All-atom force fields treat every individual atom in the system explicitly. United-atom force fields do not treat every individual atom but instead merge a few atoms together into only one interaction site. The properties of the new united-atom can be derived from the properties of the individual atoms. It is common in the treatment of aliphatic residues to merge hydrogen atoms with the carbon atoms that they are covalently bonded to. This can significantly reduce the number of interactions sites for proteins and lipid membranes and the simulations are therefore less computationally demanding. Hydrogen atoms on polar residues are often explicitly treated in order to facilitate the description of hydrogen bonding[14].

2.2. Nuclear Magnetic Resonance Spectroscopy

Elementary particles have a quantum mechanical property called *spin*. The spin of a particle corresponds to a certain degree of angular momentum of that particle. However, spin is an intrinsic property of the particle, lacking a classical analogue. Since elementary particles have spin, composite particles, such as atomic nuclei, also have a certain spin, see Table 1.

Table 1. Nuclear isotopes and their spin[31,32]

Isotope	Spin quantum number I	Natural abundance
^{1}H	$^{1}/_{2}$	~100 %
^{2}H	1	0.015 %
^{12}C	0	98.9 %
^{13}C	$^{1}/_{2}$	1.1 %
^{14}N	1	99.6 %
^{15}N	$^{1}/_{2}$	0.4 %
^{16}O	0	99.8 %
^{17}O	$^{5}/_{2}$	0.04 %

Angular momentum is a vector property but the laws of quantum mechanics prohibit knowledge of all three vector components P_x, P_y, P_z at the same time since their operators do not commute[33]. However, the magnitude P of the vector and one component, for example P_z, can be determined simultaneously. Both P and P_z are quantized, *i.e.* they can only assume discrete values, according to Eq. (22) and (23).

$$P = [I(I+1)]^{\frac{1}{2}}\hbar \qquad I = 0, \frac{1}{2}, 1, \frac{3}{2}, 2, \ldots \tag{22}$$

$$P_z = \hbar m_I \qquad m_I = -I, -I+1, \ldots, I-1, I \tag{23}$$

where I is the spin quantum number and m_I is the directional spin quantum number, $\hbar = h/2\pi$ and h is Planck´s constant. In contrast to angular momentum in classical physics, spin angular momentum gives rise to a magnetic dipole moment even for neutral particles and point particles. The spin magnetization vector $\boldsymbol{\mu}$ (or spin vector) is either parallel or antiparallel to the angular momentum vector since $\boldsymbol{\mu} = \gamma \boldsymbol{P}$, where γ is the magnetogyric ratio of the particle and γ can take positive or negative values. The measured

magnetization of a particle with spin quantum number I has $2I + 1$ different values along a defined external axis, according to Eq. (23). These spin states are degenerate when no external magnetic field is applied. When an external magnetic field is applied, the spin states will have different energy and the spin vector will align with the external field in order to minimize its energy. This is called the Zeeman effect. The energy of a magnetic moment $\boldsymbol{\mu}$ in an external magnetic field $\boldsymbol{B}$ is

$$E = -\boldsymbol{\mu} \cdot \boldsymbol{B} = -\gamma \boldsymbol{P} \cdot \boldsymbol{B} \tag{24}$$

Let us define the direction of the external field as the z-direction. The energy of a spin state is then

$$E = -\gamma P_z B = -\gamma \hbar m_I B \tag{25}$$

Since $P > P_Z$ according to Eq. (22) and (23), the spin vector cannot be parallel to the external field. Instead, the spin vector tilts relative to the external field with an angle of $\theta = \cos^{-1}\left(\frac{P_z}{P}\right)$. The magnitude of P_x and P_y are unknown and the spin vector is therefore often visualized as aligned with the perimeter of a cone centered around the z-direction. The part of the spin vector in the x,y-plane is perpendicular to the external magnetic field and the spin vector can be pictured as moving around the z-axis in a precessional motion[34]. The spin states of a particle with I = ½ in an external magnetic field is visualized in Fig. 5.

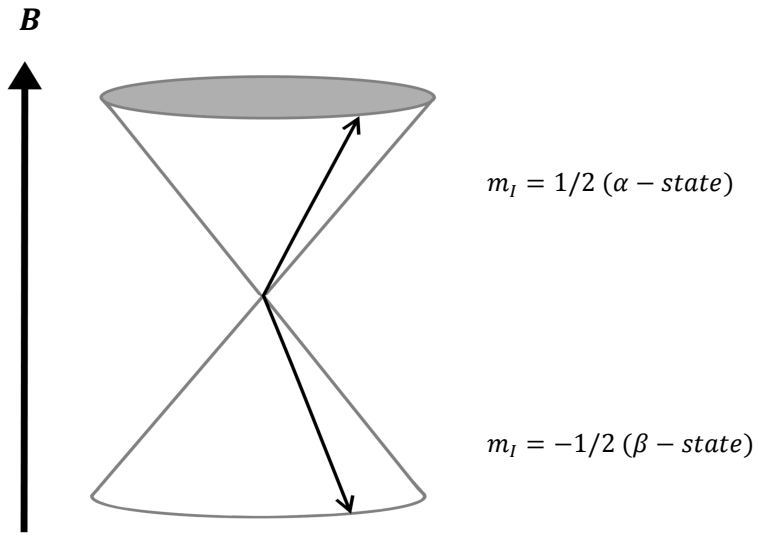

Fig. 5. The orientation of a spin vector $\boldsymbol{\mu}$ and the two possible spin states of a particle with I = ½.

In the field of Nuclear Magnetic Resonance (NMR) spectroscopy, one induces transitions among the spin states of atomic nuclei placed in an external magnetic field. The frequency condition is:

$$\mathrm{h}\nu_0 = \Delta E = |\gamma\hbar B\Delta m_I| \tag{26}$$

where the frequency ν_0 of the electromagnetic radiation corresponds to radio wave frequency. The angular frequency $\omega_0 = \nu_0 2\pi$ is known as the *Larmor frequency* and has the same value as the rate of precession of the spin vector around the z-axis. The sample is subjected to a short pulse of electromagnetic radiation in order to induce excitation of the nuclei under study. A pulse of high power and with a long duration will cause many nuclei to be excited. The pulse will also cause the spin vectors of the individual nuclei to become phase coherent in the x,y-plane. Pulses with certain strengths and durations are named after the angle that they flip the total magnetic moment vector of the sample $\boldsymbol{M} = \sum_i \boldsymbol{\mu}_i$. A 90° pulse is therefore a pulse that flips the $\boldsymbol{M}$-vector from the z-axis down to the x,y-plane. The motion of the magnetic moment vector in the x,y-plane induces a current in the nearby coils. The strength and the frequency of this current are recorded and a Fourier transform of the data yields a frequency spectra. A 180° pulse has ~twice the duration of a 90° pulse and inverts the magnetic moment in the z-direction.

Nuclear spin relaxation

The excitation of the nuclear spins by the electromagnetic pulse causes the sample to deviate from the Boltzmann distribution of the given temperature. Interactions between the nuclei under study and their surroundings cause relaxation of the spins and the sample thereby returns to thermal equilibrium. Even though the relaxation of the spins causes the observed signal to decay, the relaxation process can also be a useful source of information of the dynamics in the sample[34]. Bloch has described the relaxation process on a macroscopic level[35]. The relaxation is assumed to be exponential but the relaxation in the z-direction is allowed to occur with a different rate than in the x,y-plane. The relaxation in the z-direction is given by:

$$\frac{d\Delta M_z(t)}{dt} = -R_1\Delta M_z(t) \tag{27}$$

$$\Delta M_z(t) = M_z(t) - M_{eq} \tag{28}$$

where M_{eq} is the equilibrium magnetization in the z-direction. Solving the differential equation, Eq. (27), yields:

$$\Delta M_z(t) = \Delta M_z(0)\exp(-R_1 t) \tag{29}$$

For a frame of reference that rotates with the magnetization in the x,y-plane, the corresponding equations for the x- and y-components are given by:

$$\frac{dM_{x,y}(t)}{dt} = -R_2 M_{x,y} \tag{30}$$

and

$$M_{x,y}(t) = M_{x,y}(0)\exp(-R_2 t) \tag{31}$$

The relaxation rates R_1 and R_2 have corresponding relaxation times by the relations $R_1=1/T_1$ and $R_2=1/T_2$. The relaxation in the z-direction is called longitudinal relaxation or spin-lattice relaxation and T_1 is therefore the spin-lattice relaxation time. The relaxation in the z-direction is responsible for restoring the Boltzmann populations of the spin states. The relaxation in the x,y-plane is called transverse relaxation or spin-spin relaxation and T_2 is the corresponding relaxation time. The spin-spin relaxation is responsible for the loss of signal due to dephasing of the spin vectors in the x,y-plane.

T_1 can be measured by the inversion recovery method utilizing the pulse sequence

$$[180° - \tau - 90° - (Detection) - T_d] \tag{32}$$

where the time delay T_d is added in order to let the system relax back to the Boltzmann populations between each acquisition. T_2 can be measured by the spin-echo pulse sequence

$$\left[90°_x - \tau/2 - 180°_y - \tau/2 - (Detection) - T_d\right] \tag{33}$$

T_2 is inversely related to the spectral peak-width, *i.e.* short T_2 give broad peaks. However, the external magnetic field is often slightly inhomogeneous, which leads to a varying field strength over the sample volume. This adds to the transverse relaxation and T_2 measured from the peak widths is therefore often shorter than T_2 from a spin-echo measurement[31,34].

While the Bloch equations are macroscopic, a microscopic spin relaxation theory is provided by the works of Bloch-Wangsness-Redfield[36,37,38] (BWR). Even though it is possible to fully treat spin relaxation by quantum

mechanics, the simpler semi-classical approach of the BWR theory has proven to be very useful. The spin (spins) under study is then treated quantum mechanically but the surroundings are treated classically. The weak coupling between the surroundings and the spin system is the source of the observed spin relaxation. A number of different relaxation mechanisms for nuclear spins exist. Relaxation mechanisms for nuclei with $I = \frac{1}{2}$ are based upon fluctuating magnetic fields that originates from the thermal motion of the molecules. However, nuclei with spin quantum number $I \geq 1$, can also relax *via* the quadrupolar mechanism, which usually dominates over the other mechanisms. Nuclei with $I \geq 1$ have an electric quadrupole moment, in addition to the magnetic dipole moment. The electric quadrupole moment can be visualized as two electric dipole vectors that are positioned back-to-back. The magnetic dipole moment induced by the spin of the nucleus is parallel or at a right angle to the electric quadrupole[34]. The electric quadrupole of the nucleus interacts with the electric field gradient components of the surroundings, $\frac{\partial^2 V}{\partial i \partial j}$ where $i,j = x,y,z$ and V is the electrostatic potential at the position of the nucleus. The electric field gradient originates primarily from the molecule containing the nuclei under study. The electric quadrupole moment will therefore couple with the molecular frame while the spin vector couples with the external magnetic field. Thermal tumbling of the molecule may therefore induce spin relaxation *via* the quadrupolar mechanism.

The Hamiltonian of the spin system can be written as: $\mathcal{H} = \mathcal{H}_0 + \mathcal{H}_1(t)$, where $\mathcal{H}_0$ is the time-independent Zeeman interaction. $\mathcal{H}_1(t)$ is the stochastic time-dependent perturbation on the spin system that originates from the surroundings. $\mathcal{H}_1(t)$ will differ depending upon the relaxation mechanism under study. If we neglect other interactions than the quadrupole interaction, $\mathcal{H}_1(t)$ contains the electric field gradient components, spin operators and physical constants, such as the quadrupole moment of the nucleus. The electric field gradient will fluctuate with the molecular tumbling and this movement is responsible for the time-dependence of $\mathcal{H}_1(t)$. A correlation function $C(\tau)$ can be defined as

$$C(\tau) = < \mathcal{H}_1(t)\mathcal{H}_1(t+\tau) > \tag{34}$$

The correlation function will decay with increasing τ with a characteristic time constant τ_c, called the correlation time. The correlation time is defined as

$$\tau_c = \int_0^\infty \frac{C(\tau)}{C(0)} d\tau \tag{35}$$

The correlation time and the shape of $C(\tau)$ are indicative of the rate of fluctuations of the interaction $\mathcal{H}_1$ between the spin system and the surroundings. The frequency components of these fluctuations can be extracted by performing a Fourier transform of $C(\tau)$. We define the spectral density $J(\omega)$ as

$$J(\omega) = \int_{-\infty}^{\infty} C(\tau) e^{-i\omega\tau} d\tau \qquad (36)$$

The spectral density at the site of the nucleus represents the frequencies of electromagnetic radiation that is available for inducing transitions between the spin states. The function $J(\omega)$ will contain frequencies up to $\omega \sim 1/\tau_c$, where it quickly declines. The spectral density vs. log(ω) is almost flat for lower frequencies, $\omega \ll {}^{1}/_{\tau_c}$. This is the *extreme narrowing regime*, defined as $\omega^2\tau_c^2 \ll 1$. Since the rate of the molecular tumbling affects τ_c, the range of frequencies included in $J(\omega)$ will also be affected by the rate of the molecular tumbling. However, it can be shown that the area of the spectral density is unaffected by a change in τ_c. This causes $J(0)$ to increase with increasing τ_c. These features of $J(\omega)$ are illustrated in Fig. 6.

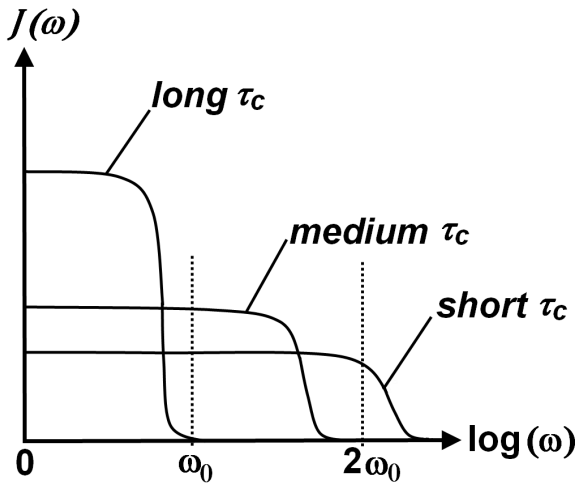

Fig. 6. The spectral density $J(\omega)$ for three different τ_c.

Spin-lattice relaxation induces transitions among the available spin states. This process transfers energy from the spin system to the surroundings and it requires radiation of the Larmor frequency ω_0. The rate of spin-lattice relaxation will therefore depend upon the amplitude of the spectral density $J(\omega)$ at $\omega = \omega_0$. Since more than one transition may be induced by the perturbation, higher frequencies such as $\omega = 2\omega_0$ may also affect the spin-lattice relaxation rate. The spectral density at the Larmor frequency $J(\omega_0)$ will be low for both long τ_c and for short τ_c, with a maximum at intermediate τ_c, as illustrated in Fig. 6. The spin-lattice relaxation rate R_1 therefore has a maximum at a certain molecular tumbling rate. Spin-spin relaxation is responsible for dephasing of the spins in the x,y-plane. This process does not involve exchange of energy between the spin system and the surroundings. The spin-spin relaxation rate therefore depends upon $J(0)$ as well as on $J(\omega_0)$ and $J(2\omega_0)$. This causes the spin-spin relaxation rate R_2 to increase with increasing τ_c, *i.e.* R_2 increases when the molecular tumbling rate is decreased by a lower temperature or by the introduction of a protein surface for example. The spectral densities $J(0), J(\omega_0), J(2\omega_0)$ are equal in the extreme narrowing regime. This has the effect that $R_1 = R_2$ for short τ_c but $R_1 < R_2$ when τ_c is long[33,34,39], see Fig. 7.

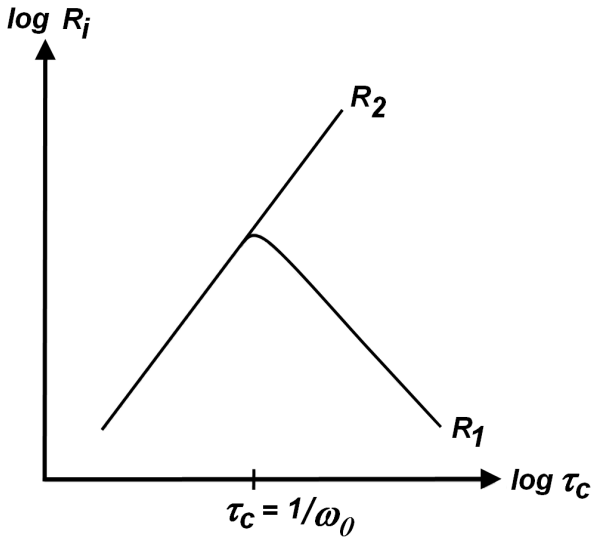

Fig. 7. Dependence of the relaxation rates on the correlation time τ_c.

The link between NMR spectroscopy and MD simulations

MD simulations are based upon classical physics and do not include quantum mechanical properties of atoms such as spin. One might therefore incorrectly assume that MD simulations cannot aid in the analysis of NMR experiments. In fact, there can be a transfer of information from NMR to MD as well as in the opposite direction. The link that joins the two methods is the dynamics of the studied system. Nuclear spin relaxation is induced due to the fluctuations of electromagnetic fields when the molecules diffuse, as seen in the correlation function $C(\tau)$ of Eq. (34) and the spectral density of Eq. (36).

The relaxation rates R_1 and R_2 measured by NMR can be interpreted in terms of molecular motion by MD simulations of the same molecular system. MD simulations can be used to calculate motional correlation functions for individual molecules, for example at different locations in the system, such as solvent in the bulk phase versus solvent near a surface. This microscopic information can be used to disentangle the experimentally obtained spin relaxation rates that are ensemble averages of the whole macroscopic system. NMR can therefore contribute with the accuracy of macroscopic experiments and the longer timescales that are possible to study, while MD simulations supply information on a molecular level.

3. The Research Field of Chemical Denaturation

The long term aim of research in the field of chemical denaturation is to explain the molecular mechanism behind the denaturant-induced decrease in the thermodynamic stability of proteins. However, connecting detailed molecular properties with thermodynamic stabilities is difficult. The complexity of such a large scale process as protein unfolding is high. There is also a very large difference in the time scale of the molecular events in the solvent that induces the unfolding and the unfolding process itself. The logical path between molecular properties and free energies is too long to be covered in one step. One should therefore first explain the affect of urea on free energies in terms of other thermodynamic properties such as enthalpies and entropies that are more closely related to the established experimental facts. When such a connection has been found and understood, the next step is to link these results to molecular properties and to understand the mechanism of urea in greater detail.

3.1. The Thermodynamics of Protein – Urea Systems

Denaturation curves

The effect of urea is general, *i.e.* all proteins are destabilized by the addition of urea, but in order to invert the populations of folded versus unfolded protein, very high concentrations of urea, up to 9 M, are usually needed. This strongly indicates that the interaction between urea and the proteins are weak. Unfortunately, a weak interaction is more difficult to study than a strong interaction. The concentration of urea that is needed to denature a protein, depends on the type of protein. Lysozyme from hen egg white cannot in a practical way be unfolded by urea at physiological pH and room temperature since very high urea concentrations are needed[40]. Anyway, the stability of lysozyme is lower in a urea solvent than in water even if complete unfolding is not reached. Studies have also shown that some proteins retain residual structure when they have been unfolded in urea[41,42,107].

The amount of urea that must be added to a protein – water solution in order to unfold a certain protein depends on the stability of the protein in water, $\Delta G_{F\rightarrow U}^{o,H2O}$, as well as on the degree of dependence of $\Delta G_{F\rightarrow U}^{o}$ on the urea concentration. The concentrations of the folded and the unfolded protein at a specific urea concentration can be measured by for example circular dichroism or fluorescence spectroscopy[43,44]. The stability of the protein at that specific urea concentration can then be calculated by using Eq. (2) and (3). If the protein contains one of the fluorescent amino acids tryptophan (Trp), tyrosine (Tyr) or phenylalanine (Phe), these can be used as internal probes for fluorescent spectroscopic measurements. Otherwise, external fluorescent probes must be attached to the protein. Tryptophan is the most popular of the internal probes since the quantum yield is high, which causes the fluorescence intensity to be high. In addition, the fluorescence intensity of tryptophan is very sensitive to the molecular environment, which makes it a good probe of structural changes in the protein. Tryptophan is hydrophobic and is therefore often located in the core of the protein. The amount of solvent contact of the residue is likely small in the folded state but will increase during unfolding. When the molecular environment of an amino acid changes, the fluorescence intensity of that amino acid will change as well. From the graph of fluorescence intensity as a function of the urea concentration, the concentrations of the folded and the unfolded protein can be calculated. The result of a fluorescence experiment of hen egg white lysozyme is displayed in Fig. 8. A plot of the unfolding Gibbs free energy $\Delta G_{F\rightarrow U}^{o}$ as a function of the urea concentration is called a *denaturation curve.* The corresponding denaturation curve of Fig. 8 is displayed in Fig. 9.

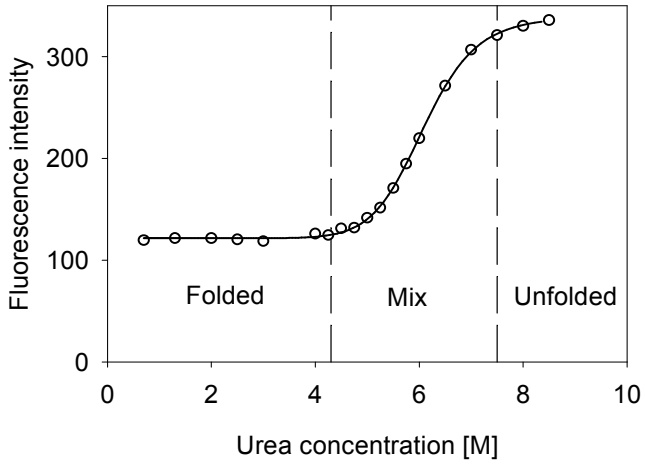

Fig. 8. Denaturation curve of hen egg white lysozyme at pH 3 as obtained by fluorescence after excitation at 280 nm and emission at 360 nm.

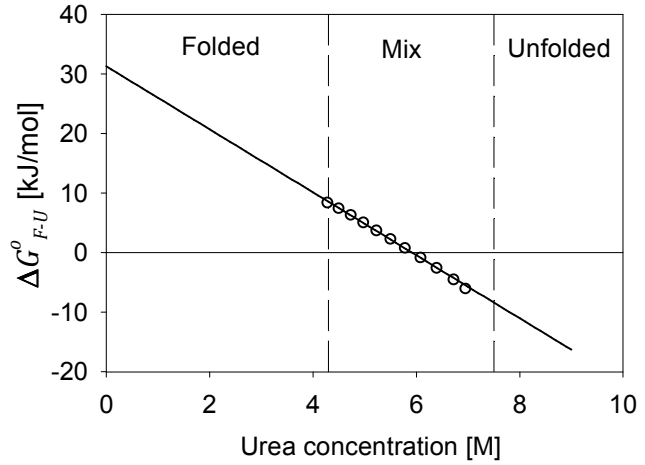

Fig. 9. Gibbs free energy of unfolding versus urea concentration for hen egg white lysozyme at pH 3. The data is fitted by a linear function according to the Linear Extrapolation Model. The protein stability in water is found to be ~ 31 kJ/mol.

The stability of the protein at low urea concentrations as well as at high urea concentrations cannot be extracted since the very low concentrations of the unfolded and the folded protein creates large uncertainties in the

equilibrium constants at those urea concentrations. The protein stability in pure water, $\Delta G_{F\rightarrow U}^{o,H2O}$, is an interesting property to measure in protein research. Unfortunately, this property cannot be extracted by other means than an extrapolation of the denaturation curve to zero urea concentration. Several theoretical models have been developed in order to make the extrapolation as correct as possible. These models are based upon varying amounts of empirical evidence and thermodynamic arguments. The simplest but also the most widely used model is the *Linear Extrapolation Model*[45]. It assumes a linear relationship between the free energy of unfolding and the denaturant concentration. The stability of the protein in water can then simply be found by linear regression of the experimental data and extrapolating to zero denaturant concentration. This model therefore does not require any additional data other than the denaturation curve, but does not give any insight into the denaturation mechanism either. The slope of the fitted line is the so-called m-value, $m = -\frac{\partial \Delta G_{F\rightarrow U}^{o}}{\partial [Urea]}$, and represents the efficiency of the denaturant in destabilizing that particular protein. The m-value has been shown to be proportional to the increase in the solvent accessible surface area (SASA) of the unfolded protein as compared to the folded protein[46]. Despite the simplicity of this model, it yields similar values of $\Delta G_{F\rightarrow U}^{o,H2O}$ as those obtained from thermal denaturation[45], at least for urea denaturation. However, some denaturation curves are not linear for low urea concentrations[47] and are better fitted with a quadratic model for instance[48].

The *Transfer Model (Tanford´s Model)*[73] is based uon experimental data of the free energies of transfer of amino acids from water to a denaturant solution. The amino acid composition of the protein as well as estimations of the SASA of the amino acids in the folded protein versus in the unfolded protein, are needed in order to extract the free energy of unfolding in water. The *Denaturant Binding Model*[49] links the effectiveness of a denaturant to preferential binding of this denaturant to the protein surface in the folded and the unfolded state.

Among these three models, linear extrapolation always gives the smallest estimated values of $\Delta G_{F\rightarrow U}^{o,H2O}$. The difference is small for urea but larger for guanidinium chloride. Since guanidinium chloride is a salt, the deviation from simple thermodynamics relationships may be due to electrostatic effects, such as screening of the protein charges[50,51]. Urea is considered to be more reliable for denaturation studies than guanidinium chloride. Other models than the three mentioned here have been proposed as well[52,53,54].

It is possible to extract $\Delta G_{F\rightarrow U}^{o,H2O}$ without using denaturants. Thermal denaturation of proteins by Differential Scanning Calorimetry (DSC) is

commonly used to gain knowledge about the thermodynamics of unfolding of the protein under study[55]. By sweeping the temperature of the sample compartment containing the protein solution, the melting temperature T_m is found at which the protein unfolds. The enthalpy change ΔH_m of the unfolding process at T_m can be extracted, as well as the heat capacity change, ΔC_p. These data can then be used to calculate $\Delta G_{F\to U}^{o,H2O}$ at an arbitrary temperature by making use of the Gibbs-Helmholtz equation:

$$\Delta G_{F\to U}^{o,H2O}(T) = \Delta H_m^o \left(1 - \frac{T}{T_m}\right) + \Delta C_p[T - T_m - T\, ln(T/T_m)] \qquad (37)$$

As for the analysis of denaturation curves, the extrapolation introduces uncertainties in the value of $\Delta G_{F\to U}^{o,H2O}$. However, comparisons of protein stabilities obtained by DSC and chemical denaturation show that they are in agreement, within the experimental uncertainties of the two methods[45,56].

Experimental studies of the thermodynamics of urea

In order to understand the destabilizing effect of urea on the folded protein, studies of the thermodynamics of protein – urea solution systems are essential. However, first it is necessary to understand why proteins fold in water. In a simple view of folding, two terms favor the folded state and one term favors the unfolded state. The unfolded protein has more solvent contact then the folded protein. Protein – water interactions are therefore replaced by protein – protein and water – water interactions during folding. These changes will in general decrease the enthalpy of the system and this term therefore favors the folded state. The other term that favors the folded state is the *hydrophobic effect*. The non-bonded interactions between water and hydrophobic side chains are weak, which increases the enthalpy of the water. In addition, the weak interactions also lead to a decrease in the entropy of water since the conformational flexibility of the water around hydrophobic solutes becomes restricted. Therefore, there are both enthalpic and entropic driving forces that lead to the clustering of hydrophobic side chains in folded proteins. The temperature dependence reveals that the hydrophobic effect is dominated by entropic driving forces at room temperature but that enthalpic driving forces make significant contributions at higher temperatures[57]. The term connected with the change of interactions during folding and the hydrophobic effect is thought to contribute equally to the stability of proteins.

The term that favors the unfolded state is the conformational entropy of the protein. The entropy of the protein decreases during folding, since the conformational flexibility is greatly reduced in the folded state as compared

to the unfolded state. In total, the terms that stabilize and destabilize the folded protein are both large and almost equal. The net protein stability is therefore often very small[58].

We now return to the discussion of thermodynamics of proteins - urea solutions. However, due to the complexity of such systems, proteins have in some studies been replaced by model compounds or individual amino acids. When Nozaki and Tanford measured the free energy of transfer of eleven amino acids from water to a urea solution in the sixties, they found that nine of the amino acids had a negative transfer free energy[59]. Only the smallest amino acids glycine and alanine had positive transfer free energies. This result indicates that both polar and hydrophobic amino acids contribute in the unfolding and also that the size of the solute molecule might be important for the affect of urea. Due to the importance of the hydrophobic effect to the stability of proteins, a natural subject of investigation is the interaction of urea with hydrophobic solutes. Wetlaufer et al.[60] measured transfer free energies of hydrocarbons and discovered that relatively large hydrocarbons, such as propane and butane, had negative transfer free energies from water to urea but very small hydrocarbons, such as methane and ethane, had positive free energies. This result shows that the hydrophobic effect may be decreased in urea but the relative importance is not unveiled. Several MD simulation studies[61,62,63,88] have also found that the interaction between a hydrophobic solute and a urea solvent depends on the size of the solute. A theoretical treatment of this effect by Graziano could explain both the dependence on the size of the solute[64] and the temperature dependence of the transfer free energy[65] in the data of Wetlaufer et al[60]. It was found that cavity formation entropy has a larger negative value in a urea solution than in water. This effect dominates for small hydrophobic solute molecules. However, the vdw interaction between the solute and the solvent is more attractive in the urea solution than in water and this effect dominates for large hydrophobic solutes. This means that large hydrophobic solutes can be favorably solvated in a urea solvent due to the enthalpic driving force of solute – solvent vdw interactions. The favorable vdw interactions with a urea solution were explained by the high packing density of urea solutions, the high polarizability and the large dipole moment of the urea molecule[64]. The free energy of cavity formation has been confirmed to increase with urea concentration in a similar theoretical analysis of the transfer experiments[66].

The transfer free energy study performed by Robinson and Jencks[67] concerned a model compound that resembles a peptide backbone, rather than hydrophobic side chains. The transfer free energy from water to a urea solution was negative also for this polar compound. However, it should be noted that the negative free energy is realized in different ways for two types

of compounds. Both the enthalpy and the entropy of transfer of large hydrocarbons from water to urea are positive, but the corresponding enthalpy and entropy of transfer of the polar backbone compound are negative[60,67]. This has been confirmed in other studies[68],[69]. Interestingly, the studies of Graziano[64,65] shows that the transfer of hydrocarbons from water to a urea solution or to a guanidinium chloride solution includes a large amount of hydrogen bond restructuring between solvent molecules. This effect is connected with large positive enthalpic and entropic terms that are included in the experimentally measured transfer thermodynamics. However, it can be shown that the entropic term $-T\Delta S°$ and the enthalpic term of hydrogen bond restructuring exactly cancel each other for solutions where the solute – solvent interactions are weak as compared to the solvent – solvent interactions. This applies to a urea solution with a hydrocarbon solute and the effect of hydrogen bond restructuring can therefore be removed from the calculation of the free energy. It is then found that the transfer of hydrocarbons from water to a urea solution is characterized by a negative enthalpy term and a negative entropy term. Transfer of both hydrocarbons and the backbone compound are therefore driven by an enthalpic driving force. The main results of Graziano are supported by an MD simulation study of neo-pentane solvation[70]. The results are also in agreement with a calorimetric study of the interaction between urea and three globular proteins[71]. The addition of urea from 0 M to 2 M was seen to promote protein unfolding by decreasing the enthalpy of unfolding. The entropy of unfolding was also decreased but the effect on the enthalpy was larger and urea therefore decreased the Gibbs free energy of unfolding. The results of another calorimetric study of five globular proteins were similar[72]. The enthalpies of interaction between urea and the proteins were exothermic for all proteins and the unfolding was exothermic in urea, in contrast to the endothermic unfolding in water.

3.2. Proposed Mechanisms of Urea-Induced Denaturation

A number of mechanisms of urea-induced denaturation have been proposed. These different mechanisms have been categorized according to whether urea interacts and destabilizes proteins by itself, the so called *direct mechanism,* or if urea instead acts on water and thereby change the properties of the water into a solvent that destabilizes proteins. This is called the *indirect mechanism*. From these two classes, three proposed mechanisms have gained the most attention with a number of papers in support of, or against, each mechanism.

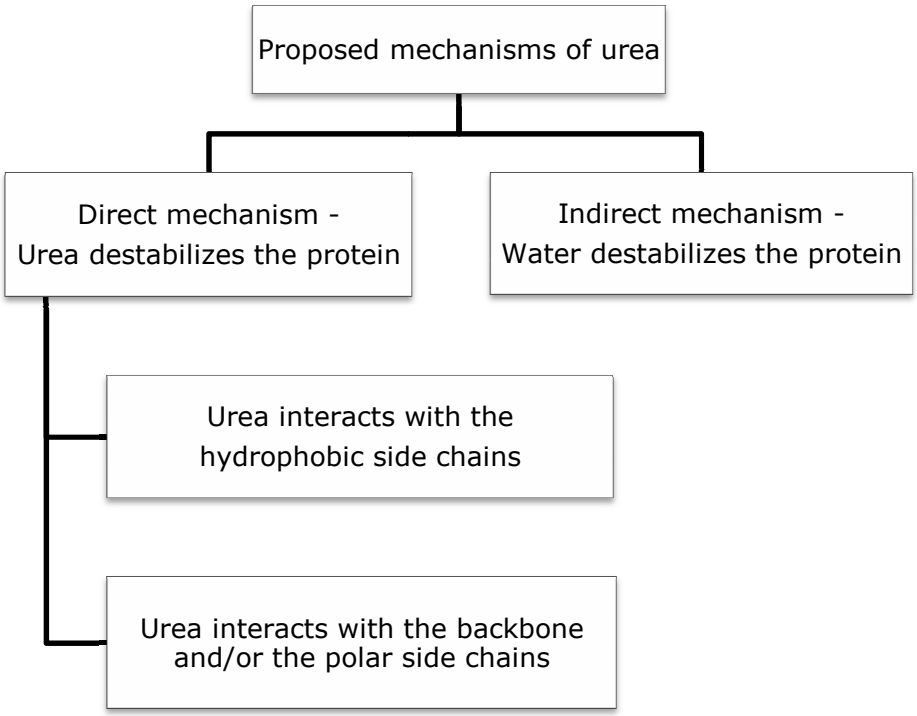

Fig. 10. Schematics of three proposed mechanisms of urea-induced protein denaturation.

Direct mechanism

In the class of the direct mechanism, one finds the proposed interaction of urea with hydrophobic side chains, which is said to reduce the hydrophobic effect. The study of Wetlaufer et al.[60] can be interpreted as to support this mechanism, even though the interaction between urea and small hydrocarbons was found to be unfavorable. Similarly, the proposed interaction between urea and the protein backbone also classifies as the direct mechanism. This mechanism is supported by the transfer free energy study performed by Robinson and Jencks[67] for example, but it is also frequently noted in the literature that the similarity of the urea molecule with the peptide bond of the protein backbone could facilitate such an interaction.

The question of whether urea destabilizes proteins mainly by interactions with the hydrophobic side chains or with the backbone is the subject of an ongoing debate. However, it should be noted that the early studies of the transfer free energy of model compounds indicate that both interactions with

the hydrophobic side chains and the backbone should contribute to the destabilizing effect of urea. The conclusions of Tanford[73] and of Wetlaufer et al.[60] were that the interactions between urea and the hydrophobic side chains and with the backbone make equal contributions for the effect of urea on proteins.

Indirect mechanism

Some controversy exists about the structure of the binary urea – water solution. The papers of Schellman[74], Kresheck - Scheraga[75] and Stokes[76] constitute the *SKSS model* of the urea solution structure. They proposed that the water structure is unchanged by urea but that urea itself forms dimers and oligomers due to hydrogen bonds between the -NH and –CO groups, similar to the hydrogen bonded secondary structures found in proteins. Papers in support of the SKSS model exist, see for example Ref. 77. However, the rotational correlation time of urea in water solution has been obtained by NMR and it indicates that the majority of urea exists in the monomer form in water solution[78]. A study of the urea solution structure by using Raman spectroscopy did not find any evidence for urea dimers[79].

Another model of the structure of urea – water solutions, the *Frank-Franks (FF) model*[80], forms the basis of the indirect mechanism of urea-induced protein denaturation. According to this model, urea decreases the structure of water, *i.e.* urea acts as a *chaotrope*. The ordering of water close to hydrophobic surfaces is therefore possibly reduced by urea, thereby making water better at accommodating hydrophobic solutes. The ideas of this mechanism originate from a theoretical analysis[80] of the transfer study of hydrocarbons performed by Wetlaufer et al[60]. In the employed theoretical model, water is treated as composed of two different phases, one bulky and highly hydrogen bonded structured phase and one dense phase with less structure. Urea is pictured as being soluble only in the dense, unstructured water phase, thus lowering the chemical potential of that phase. In order to maintain equilibrium with the structured water phase, the equilibrium is shifted towards the water phase with less structure, *i.e.* urea is a water structure breaker. Hydrocarbons are said to increase the structure of water but this effect can be counteracted by the structure breaking effect of urea and there is therefore a gain in entropy associated with the transfer of hydrocarbons from water to a urea solution, as experimentally observed[60].

Studies aiming at investigating the proposed water structure breaking effect of urea have been conducted. As for the SKSS model, some studies show results in accordance with the FF model and the indirect mechanism of chemical denaturation, see for example Ref. 78,81,82. In contrast, some studies find that urea increases the water structure[85,83] and propose that this

can also explain the denaturation of proteins. Even though this discussion has not been settled, it seems that the present view is that urea does not alter the water structure to any high degree. This conclusion is supported by a number of studies[3,61,77,88,105]. If this is true, urea does not denature proteins by the indirect mechanism.

3.3. MD Simulation Studies of Chemical Denaturation

The MD simulation technique has been utilized in studies of the structural properties[61,83,84], the dynamics[85,86] and the solubility properties[61,62,84,87,88] of the urea / water mixture. MD simulations have also been used in studying the effect of urea on peptides and model compounds[89,90,91,92,93,94,95] as well as on proteins[96,97,98,99,100,101,102,103,104,105,106,107,108]. Some studies were published as early as the 1980s but the results from those studies are vague due to the very short simulations (ps - ns) as compared to the timescale of protein unfolding (μs – ms). Simulations long enough to show the majority of an unfolding trajectory have only been possible in the last few years. At present, simulations of the complete unfolding of small to medium sized proteins are possible but elevated temperatures are often needed in order to accelerate the unfolding.

A clear result from the MD simulation studies is that urea has a higher concentration close to the protein surface than in the bulk phase, see for example Ref. 89, 90, 94, 95. In the simulations of Stumpe and Grubmüller, the concentration of urea was found to be especially high at the hydrophobic amino acids and water preferentially solvated the charged amino acids. They argue that this effect is due to electrostatic interactions, rather than Lennard-Jones interactions or entropic factors. Unfortunately, the cutoff in the analysis of the force field energies was short, which raises doubts about the results. Still, in additional simulations[107] they found that a urea model with downscaled charges denatures proteins much faster than the urea model with the original charges. Urea with upscaled charges even seemed to stabilize the protein. It was therefore suggested that “apolar urea-protein interactions, and not polar interactions, are the dominant driving force for denaturation”. The interaction between urea and the hydrophobic parts of the protein was also found to impede the hydrophobic collapse of partially unfolded proteins[106].

In contrast, the research group of Thirumalai has published a number of papers[90,91,95] where they argue that urea denatures proteins primarily by the direct mechanism but *via* electrostatic interactions with the protein backbone or polar side chains. However, they incorrectly assume that the

stabilization of methane in a urea solution as compared to in water (as seen in their calculations of the potential of mean force PMF) apply to larger hydrophobic solutes as well. In addition, the negligible effect of urea on the PMF of an ionic pair is not significantly discussed[91]. They note that urea accumulates near the protein surface, as seen in radial distribution functions (RDFs). Significant hydrogen bonding can also be seen between the peptide and the urea molecules and this is interpreted as a main cause of the effect of urea on proteins[90]. However, the cause-and-effect relation between the accumulation of urea near the peptide and the number of hydrogen bonds is not investigated further. The relation between the hydrogen bonding and the protein destabilization is also assumed without more analysis. In Ref. 95, the unfolding equilibrium of a hydrocarbon chain is studied in water and 6 M urea. Strangely, it was found that the folded structure of the hydrocarbon was destabilized by introducing charges of different signs at the ends of the hydrocarbon chain. This result can perhaps be traced to inadequate sampling due to the limited simulation lengths of 3 - 4 ns.

As mentioned in the section regarding experimental studies of the thermodynamics of urea, support has been found that the dependence of the transfer free energy upon the solute size is caused primarily by van der Waals interactions. This is in agreement with an MD simulation study of ion solvation in urea solutions[88]. They conclude that enthalpic interactions rather than entropic cause the dependence on solute size. Furthermore, these results gain support from a study[105] of MD simulations of Lysozyme in a urea solution and of MD simulations[92] of hydrophobic model compounds. In these studies, the non-bonded interactions were divided between the Lennard-Jones and the electrostatic constituents. It was found that the Lennard-Jones interaction between the protein and urea was more attractive than between the protein and water. On the other hand, no support could be found for the indirect mechanism. Both studies conclude that the Lennard-Jones interaction between protein and urea is likely to be the main cause for the protein denaturation observed in their MD simulations.

The relative importance of electrostatic and Lennard-Jones interactions for chemical denaturation in MD simulations was investigated in a recent paper[108]. Both electrostatic and Lennard-Jones interactions were reported to be more favorable between proteins and a urea solvent as compared to between proteins and water. Unfortunately, the short denaturation processes (< 30 ns at 325 K) and the very large difference in the potential energy of urea between the bulk phase and the protein solvation shell (a factor of 2) raises doubts about the setup and the analysis of the simulations.

When reviewing the MD simulation studies on chemical denaturation, it becomes apparent that it has been unclear what observable to calculate from the simulation data in order to understand the unfolding. Many studies describe the unfolding trajectory visually and in terms of structural parameters of the protein. However, only one or a few replicate simulations can be performed and analyzed due to the limited computer performance available. It is then uncertain if the analyzed trajectories are representative of all possible unfolding pathways. In addition, these systems are not in equilibrium. If we are to connect the experimentally observed thermodynamic properties of unfolding with results of simulations, the simulation systems must be kept in equilibrium and the calculated properties must be averaged over many replicate simulations.

Several papers[89,93,96,98,101] include an analysis of the hydrogen bonding between solvent molecules and between urea / water and the protein. Properties such as the life-times and the bond lengths of these hydrogen bonds are calculated. Also for this type of analysis, it is unclear how to connect the calculated properties with the destabilization of the protein without introducing a high degree of assumption.

As was written in the beginning of Chapter 3, the long term goal of the research concerning chemical denaturation is to explain the molecular mechanism behind the denaturant-induced decrease in the thermodynamic stability of proteins. In my opinion, this cannot be done in one step. The effect of urea on the thermodynamic properties of protein – urea solution systems must be established first. Experimental techniques such as DSC and ITC are needed in thermodynamic studies, but they should be accompanied by MD simulations so that the various enthalpic and entropic terms can be separated, in order to attain a greater level of detail.

4. Results

Paper I concerns the effect of urea on the protein Chymotrypsin Inhibitor 2 (CI2), as seen by MD simulations. The study takes a thermodynamic approach by comparing the interaction energies between the protein and water and between the protein and a urea solvent. In Paper II we use a combination of MD simulations and NMR relaxation experiments as tools in the study of the structure and the dynamics of urea in the solvation shell of hen egg white lysozyme. While Paper I has a thermodynamic approach to the affect of urea on CI2, the focus of Paper III is instead the effect of urea on the kinetics of unfolding processes on a local level in CI2, as studied by MD simulations. CI2 was chosen for these studies since it is a small and well-known protein, having both an α-helix and β-strands, see Fig. 11. Lysozyme was chosen due to experimental suitability. Both proteins are assumed to represent general proteins and the affect of urea on these proteins are therefore assumed to be similar to the affect on other proteins.

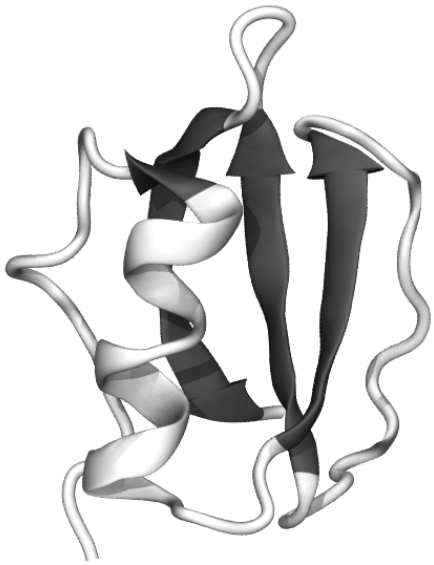

Fig. 11. Cartoon representation of Chymotrypsin Inhibitor 2.

Paper I

MD simulations of CI2 in water as well as in 10 M urea were performed. The systems must be in equilibrium in order to extract the effect of urea on quantities of equilibrium thermodynamics. The folded structure of CI2 in a 10 M urea solution is not an equilibrium system since the protein will undergo unfolding as a response to the presence of urea. We therefore restricted the protein to the folded state by employing positional restraint potentials on the α-carbons. The restraints will counteract the influence of urea and keep the system in a forced equilibrium state when the protein is dissolved in 10 M urea. The restraint potentials will necessarily affect the folded protein by reducing the phase space available to it. In order to be able to compare the simulations in urea and in water, it was therefore necessary to employ the same restraints on the protein in water as well. The use of positional restraints may influence the absolute values of the interaction energies but the flexible side chains will help to keep this effect small and, more importantly, the trend in the data is still visible. A positive side effect of the reduction of the phase space of the folded state is that the sampling is facilitated.

The protein atoms were classified as belonging to either the backbone, the hydrophilic side chains or the hydrophobic side chains. MD simulations where CI2 was solvated by either water or by 10 M urea were performed and compared with respect to the protein – solvent interaction energies. The change in the internal energy of this system due to protein unfolding can be written as a sum of three terms as in Eq. (38).

$$\Delta U^o = \Delta U^o_{protein} + \Delta U^o_{solvent} + \Delta U^o_{protein-solvent} \qquad (38)$$

It is likely that urea affects all three of these terms but to a different extent. The third term, $\Delta U^o_{protein-solvent}$, was extensively studied in Paper I with a shorter analysis of $\Delta U^o_{solvent}$. The results showed that an enthalpic driving force for urea-induced denaturation exists. The interaction energy between the solvent and the protein decreased by as much as 12 per cent in the 10 M urea solvent as compared to in water. In the interplay between protein – protein, solvent – solvent and protein – solvent interactions, the decrease in the protein – solvent energies will favor an increased protein - solvent contact by an increase in the protein SASA. All three parts of the protein; the backbone, the hydrophilic and the hydrophobic side chains, had a more favorable interaction with the urea solvent than with water. The protein surface that opens up to solvent during unfolding will have similar properties as compared to the folded protein, but perhaps with larger fractions of backbone and hydrophobic surface. The presence of urea is therefore likely to cause $\Delta U^o_{protein-solvent}$ to decrease. From the viewpoint of protein –

solvent interaction energies, all parts of the protein contribute to the unfolding of the protein. When separating the protein – solvent interaction energies into its constituents, electrostatic interactions and Lennard – Jones interactions, it was found that both the relative and the absolute decreases in the electrostatic energies were small while the decreases in the Lennard – Jones energies were large. The origin of the decrease in the protein – solvent energies was therefore the ability of the urea solution to form attractive Lennard – Jones interactions with all parts of the protein.

When shifting the viewpoint from the protein to the solvent, it was found that water molecules in the protein solvation shell had higher interaction energies relative to bulk water but urea molecules had lower interaction energies relative to bulk urea. This creates an energetic driving force for the replacement of water by urea at the protein solvation shell. The enrichment of urea in the solvation shell has been observed[87,88,92,93] but can also be attributed to the gain in entropy of the system when several restricted water molecules in the solvation shell are replaced by one large urea molecule, as commonly noted in the literature.

It is likely that the solvation shell energy relative to bulk solvent energy is changed when urea is added. However, this change was found to be small relative to the uncertainties in the calculated energy values. The effect of urea on $\Delta U^o_{solvent}$ could therefore not be calculated.

The intramolecular protein energy, $\Delta U^o_{protein}$, is a function of the protein structure but it is unaffected by the solvent, except from changes in the permittivity of the solution. The effect of urea on $\Delta U^o_{protein}$ is therefore small as long as we compare the same folded and unfolded protein states in both solvents. However, it is likely that urea does affect which structures that are incorporated into the folded and the unfolded state. It has been suggested that the unfolded protein states in different urea concentrations may be structurally different but thermodynamically similar[45]. Unfortunately, the unfolded state in water and the folded state in 10 M urea are difficult to study experimentally and not much are known about these states. It may be that the change in $\Delta G^o_{protein}$ and $\Delta U^o_{protein}$ when urea is added is mostly due to this effect, but the lack of information prevents us from estimating the relative importance of the protein intramolecular term in Eq. (38).

Paper II

In Paper II, we combined MD simulations with NMR spin relaxation measurements in order to investigate structural and dynamic properties of urea in the solvation shell of hen egg white lysozyme. The relaxation rate of the quadrupolar nuclei ^{14}N in the urea molecule was used as a probe to study the dynamics of individual urea molecules at the protein interface. The urea molecules that are dynamically retarded by the contact with the protein surface will experience significantly enhanced relaxation rates. The fraction of the urea solvent that is in contact with a protein is small, since the protein concentration is relatively low due to the limited solubility. However, by utilizing the fact that the molecules in the solvation shell undergo fast chemical exchange with the bulk phase, the enhanced relaxation rates of the urea molecules in the solvation shell can be seen in the relaxation enhancement of the urea molecules in the bulk phase.

The spin-lattice and the spin-spin relaxation rates of ^{14}N in urea were obtained at 100 MHz and 400 MHz magnetic field strengths from samples with or without lysozyme and urea concentrations of 3 M or 8.5 M. The results were analyzed by employing a three-site model with fractions F, B and C of urea, with different intrinsic relaxation rates of urea at each site. The F fraction corresponded to urea in the bulk solvent that did not interact with the protein. The B fraction corresponded to urea molecules that reside in the protein solvation shell but with a residence time shorter than 3 ns. The C fraction was the urea molecules that had a residence time in the solvation shell longer than 3 ns.

The results from the NMR relaxation experiments alone cannot be used to resolve all parameters of the model, since the model is underdetermined. However, by combining NMR with results from MD simulations of the same systems, a full parameter set of the model could be found that successfully describes the spin-lattice relaxation rates and gave a plausible picture of the dynamics of urea in contact with a protein surface. This approach can therefore successfully be used in the study of chemical denaturation. It was found that the dynamics of the urea molecules in the vicinity of the protein was similar to water in the same region, when the different sizes of the molecules were taken into account. The urea molecules were dynamically retarded by the protein surface but not to a higher degree than water molecules. The results did not support the hypothesis that specific urea binding sites exists on the protein[71,109,110]. Urea is instead dynamic and diffuses around the protein surface. The interaction between urea and the protein will therefore be averaged with respect to the orientation of urea and the type of amino acid.

The sample that contained lysozyme in the folded structure, solvated in 3 M urea, showed a clear field dependence and $R_2 > R_1$. This was attributed to the small C fraction of urea molecules. It could be seen from an MD simulation of the system that, at any point in time, a few (~3) urea molecules reside in pockets and grooves at the lysozyme surface with a residence time longer than 3 ns. These urea molecules have a restricted rotational motion with respect to the protein surface and the rotational averaging is therefore partly governed by the rotation of the protein - solvent complex. The rotational correlation time τ is therefore long and the extreme narrowing condition, $\omega^2\tau_c^2 \ll 1$ is not fulfilled. The relaxation rates of the sample with unfolded lysozyme in 8.5 M urea were not field dependent. It is therefore likely that the pockets and grooves on the lysozyme surface that seems to be needed for the long residence times, are absent in the unfolded protein structure. The topology of the protein surface, rather than the primary structure, determines the presence of urea molecules with long residence time. Once again we note the absence of specific urea binding sites on protein surfaces.

Paper III

In understanding the mechanism of urea-induced denaturation we require not only knowledge about the thermodynamic basis of denaturation but also how the denaturation is realized on a molecular scale. In Paper III we analyzed the affect of urea on local protein processes from a kinetic view point. After all, the molecular action of urea must occur on a local level but this manifests itself in the large effect on the kinetics of the global folding and unfolding processes. However, this mechanism has not been subjected to much research and is not well understood. One may ask what kind of local processes that are affected by urea and how they are affected. It is also not known if urea actively unfolds small protein structures or if urea instead acts by retarding the refolding of such structures.

In an attempt to understand these mechanisms, the dynamics of protein processes of different scales were analyzed in protein – water and protein – urea simulations. Very small processes such as the fluctuation amplitudes of individual backbone atoms were not affected by urea, even though the tendency for global unfolding is so much higher in the urea solvent. However, the effect of urea was clearly seen when studying larger scale processes. An intra-protein electrostatic bond between the side chains of methionine and lysine could be seen to fluctuate between the open and closed forms, both in water and in the urea solvent. Both the rate constants for the opening and the closing processes were decreased by the addition of urea. In contrast, the rupture frequencies of the hydrogen bonds of the alpha

helix and the C- and N-terminal regions were seen to be increased by urea, similar to the effect of urea on the global unfolding rate.

Based on these results, we proposed that the effect of urea on the unfolding rate of protein structures depends on whether the process is isolated or if it is triggered by the unfolding of other nearby structures. For example, the fluctuation of a side chain with a high degree of solvent contact occurs almost independently of other simultaneous processes that occur in the protein. Both the unfolding rate and the refolding rate of such a process seem to be decreased by urea, as seen in our study and also noted by Stumpe and Grubmüller[106]. The unfolding of secondary structure elements are not isolated events. They are instead triggered by, for example, unfolding of nearby side chains. Urea hinders the refolding of these side chains, which gives time for other unfolding processes to occur. This chain of events destabilizes the secondary structures and they eventually unfold. Their unfolding rate may therefore be increased in a urea solution due to the decreased refolding rate of isolated unfolding processes.

5. Discussion

This thesis is devoted to the study of urea-induced protein denaturation. The research field of chemical denaturation has been studied for a long time, with the research by Schellman[74] in the fifties as a starting point. It must be said; progress has been slow. This can perhaps be attributed to the subtle and weak interactions between the denaturants and the proteins, as seen by the requirement of very high denaturant concentrations in order to induce protein unfolding. Even in an 8 M urea solution, where ~35% of the water molecules have been replaced by urea, three tested globular proteins were far from saturated with urea[71]. Still, many studies have aimed at finding the binding constant and the specific binding sites of urea. For example, Privalov and Makhatadze[71] used calorimetric data to determine the binding constant and the number of binding sites of urea on proteins. The number of sites were then correlated with structural features of each protein in order to determine where the binding sites were located. They found that the number of sites correlated best with the number of exposed polar groups, but with the requirement that each urea molecule binds to two hydrogen bond forming groups. The correlation to the number of exposed hydrophobic groups was low. However, it must be questioned if specific binding sites can be determined when the binding constant is as low as 0.06, which gives a binding free energy of individual urea molecules of +6.9kJ/mol. We studied the dynamical properties of urea in Paper II. The results showed that the dynamical retardation of urea when it interacts with a protein surface is

approximately the same as for water. An especially strong and specific binding between urea and proteins is therefore unlikely.

In my opinion, before one searches for the details of the mechanism of urea, the thermodynamic basis of protein denaturation must be firmly established. A number of important articles with this aim were published in the sixties. The results of these studies have often been viewed as contradictory but in fact they are not. It was shown[59,60,67,73] that a urea solution interacts favorably with both hydrophobic and hydrophilic amino acids as well as with the protein backbone. The only exception was the smallest amino acids. The interaction between urea and all types of protein surfaces will therefore favor protein unfolding. The results of calorimetric studies[71,72] show that the addition of urea causes protein unfolding to become exothermic instead of endothermic. The theoretical studies of Graziano[64,65] support the view that enthalpic factors denature proteins. He concluded that the van der Waals interaction is more favorable for a hydrophobic solute in a urea solution than in water and that this term dominates for large solutes. These experimental and theoretical studies are in accord with our MD simulation results of Paper I and with other MD simulation studies[92,105].

Even though opposite results have been published for the affect of urea on the water structure, it seems that most studies support the view that urea does not to any high degree affect the water structure. The indirect mechanism can therefore be excluded from the present discussion. However, urea does change the properties of water in the sense that urea has been shown to accumulate at the protein interface, thereby releasing water molecules to the bulk phase. As noted in the discussion of Paper I, this mechanism is driven by enthalpic driving forces but perhaps also by entropic driving forces. The hydrophobic effect is entropic in nature at room temperature[57] and the negative transfer free energy of hydrophobic solutes from water to urea due to enthalpic driving forces should therefore not be interpreted as a reduction of the hydrophobic effect. If urea does reduce the hydrophobic effect, it cannot be the dominating mechanism of urea since urea-induced denaturation is enthalpic in nature[71].

Besides the hydrophobic effect, the protein conformational entropy is also a large entropic term in protein folding and unfolding. The hydrophobic effect favors the folded state and a reduction of the hydrophobic effect would therefore favor the unfolded state. However, the conformational entropy of the protein favors the unfolded state. A reduction of this term by urea would therefore favor the folded state and thereby counteract the reduction of the hydrophobic effect. In fact, urea has been proposed to reduce the term connected with the conformational entropy, due to the *excluded volume*

effect[111]. When a large solvent molecule is attached to a protein, the effective volume of that protein increases. Nearby proteins will have a smaller amount of space to move around in and the conformational entropy of those proteins will therefore decrease. This effect favors the folded state since folded proteins are restricted in their conformational freedom already before urea is added. Urea is a larger molecule than water and will therefore favor the folded state with regards to the excluded volume effect. A theoretical analysis of the excluded volume effect of urea[111] found that the effect was large. It is therefore possible that the excluded volume effect fully counteracts a possible reduction of the hydrophobic effect by urea. The addition of urea would decrease the gain in entropy during unfolding rather than increase it.

Is it possible to scale down the thermodynamic results of Paper I in order to discuss the mechanism of urea on a molecular scale? Paper I shows that the protein – solvent interaction energies decreases in the presence of urea, due to the highly negative Lennard – Jones energies between protein and urea. As noted before, several studies have found that urea is enriched at the protein surface as compared to the bulk phase. These two results indicate that the binding energy and the binding free energy between a protein and urea molecules are stronger than between a protein and water. How will the strong binding affect the kinetics of unfolding and refolding? In Paper III, we discussed the affect of urea on the kinetics of local processes. We proposed that urea increases the global unfolding rate by retaining in solution local parts of the protein that have unfolded by thermal fluctuations. This gives more time for sequential local unfolding processes to occur. Urea decreases the refolding rates rather than increases the unfolding rates of small scale processes in a protein. One could say that the mechanism of urea is passive rather than active on the local level. A stronger binding between protein and urea as compared to between protein and water seems to be in agreement with the ability of urea to decrease the refolding rates of local protein parts. Steric hindrance will prohibit refolding as long as the urea molecule is strongly attached to the protein. However, the affect of the protein - urea binding on the local unfolding rates is more complex and additional studies are required.

6. My View of the Mechanism of Urea

Both microscopic and macroscopic information is needed in order to understand chemical denaturation. Using a combination of experimental and simulation methods therefore seems the best route to take. The long simulations needed for proper sampling require fast computer hardware and software that only has been widely available for the last few years. Experiments such as transfer free energy studies and calorimetric studies can now be compared with and dissected into finer details by using computer simulations. Such an analysis has been one of the main goals with this thesis. Considering the lack of agreement in the conclusions of studies regarding chemical denaturation, I was surprised to find that a consistent view could be found. From the transfer free energy studies in the 1960s via theoretical analyses, NMR, DSC and MD simulations, results are found that support a mechanism where urea denatures proteins by not doing anything spectacular.

Based on the results of others in combination with my own, I propose the following mechanism of urea-induced denaturation. The first step in the unfolding process is the accumulation of urea at the protein interface. This process may be driven by the decrease in enthalpy of the solvent that occurs when water in the solvation shell is replaced by urea. In addition, the release of conformationally restricted water molecules from the solvation shell by the larger urea molecule may increase the entropy of the solvent.

The replacement of water with urea near the protein leads to a decrease in the protein – solvent van der Waals energy (dispersion and Debye terms). Graziano explains the favorable van der Waals interactions between a solute and urea solutions with the high packing density of urea solutions and the high polarizability and high dipole moment of the urea molecule[64]. Van der Waals interactions are not as discriminating as electrostatic interactions with respect to the nature of the amino acid. Urea therefore interacts favorably with the whole protein without the need for specific binding sites. The interaction between protein and urea is not so strong or specific that urea becomes static. Instead urea diffuses across the protein surface and should be regarded as dynamic. The decrease of the protein – solvent interaction energies induces unfolding by promoting an increase in the protein SASA. The magnitude of the urea-induced decrease in $\Delta U^{o}_{F\rightarrow U}$ and $\Delta G^{o}_{F\rightarrow U}$ will depend on ΔSASA of the entire protein.

Urea has a good hydrogen bonding ability due to having both carbonyl and amine groups. This is important in two respects. First, hydrogen bonds between the urea and the protein are necessary in order to keep the

electrostatic interaction energies between the protein and the urea solvent on the same level as between the protein and water. Even though the decreases in the van der Waals energies are relatively large, an increased electrostatic energy could counteract that effect. Secondly, hydrogen bonds between urea and water will facilitate solvation of urea to the very high concentrations needed in order to induce denaturation.

From a kinetic viewpoint, thermal fluctuations of structures within the protein will locally open up the protein and expose additional protein surface to the solvent. Binding of urea to the newly exposed protein surface may increase the rate of sequential unfolding by sterically hinder the refolding. The rate of protein folding may decrease by the same argument.

In formulating the mechanism above, I have tried to summarize and merge together the main results of the research in the field. However, papers with results and conclusions that deviate from this view exist. More research is certainly needed in order to further validate or discard the proposed mechanism. For example, understanding the affect of urea on the solvation shell energy should be a key component in future studies. If MD simulations are used in combination with calorimetric experiments, I am positive that the mechanism of urea-induced denaturation will be completely understood in the near future.

Acknowledgments

TACK!

Per-Olof "The Supervisor" Westlund – For good supervision during these five years and for all the hours you have spent working with our project. For sharing your knowledge of physical chemistry. For your conviction that research is not (only) about personal fame and fortune.

Tobias "The NMR guru" Sparrman – For assistance with my NMR experiments. You know your stuff.

Tobias "The Geek Dictionary" Sparrman – For giving lectures about the MPEG-4 compression format. For taking the time to listen to my many questions regarding thermodynamics and such. For answering a reasonable fraction of those questions.

Aatto "Simulation Guru" Laaksonen – For sharing your knowledge about computer simulations and assisting in my simulation projects. Your input was needed and I am truly grateful.

Janusz "Simulation Guru" Zdunek – For introducing me into the field of MD simulations and for your assistance in the startup phase of the project.

Erik "I can speak English!" Rosenbaum – My sentences correcting you have.

Therese "Stenkoll" Mikaelsson – For notifying me when it was time to go to the Wednesday seminar.

All my other colleagues at and around the Department of Chemistry - You have not done shit in my project but I like you anyway.

My family – För klappar på axeln och sparkar i baken.

Matilda "The Girlfriend" Carlsson –For making me see beyond problematic proteins and elusive interactions. Puss Paj!

If there are no stupid questions, then what kind of questions do stupid people ask? Do they get smart just in time to ask questions?

Scott Adams

References

[1] K. J. Laidler, M. C. King, *J. Phys. Chem.,* 1983, **87**, 2657

[2] W. Ramsden, *J. Physiol.,* 1902, **28**, xxiii

[3] J. D. Batchelor et al., *J. Am. Chem. Soc.,* 2004, **126**, 1958

[4] M. J. Lindberg et al., *Proc. Natl. Acad. Sci. USA*, 2005, **102**, 9754

[5] B. J. Alder, T. E. Wainwright, *J. Chem. Phys.*, 1957, **27**,1208

[6] J. Norberg, L. Nilsson, *Quarterly Rev. Biophys*., 2003, **36**, 257

[7] B. R. Brooks et al., *J. Comp. Chem.,* 2009, **30**, 1545

[8] D. A. Case et al., AMBER 10, *University of California, San Francisco,* 2008

[9] B. Hess et al., *J. Chem. Theory Comput*., 2008, **4**, 435

[10] Levitt, M. et al., *Comp. Phys. Comm.*, 1995, **91**, 215

[11] J. C. Phillips et al., *J. Comp. Chem*., 2005, **26**, 1781

[12] D. Frenkel, B. Smit, *Understanding Molecular Simulations: From Algorithms to Applications*, 2nd ed., ACADEMIC PRESS, San Diego, California, 2002

[13] J. Phillips et al., NAMD Tutorial, University of Illinois at Urbana-Champaign, 2009

[14] A. D. Mackerell *, J. Comput. Chem.,* 2004, **25** ,1584

[15] H. C. Andersen, *J. Chem. Phys*., 1980, **72**, 2384

[16] H. J. C. Berendsen et al., *J. Chem. Phys*., 1984, **81**, 3684

[17] S. Nosé, *Mol. Phys.,* 1984, **52**, 255

[18] W. G. Hoover, *Phys. Rev. A*, 1985, **31**, 1695

[19] M. Parrinello, A. Rahman, *J. Appl. Phys*., 1981, **52**, 7182

[20] D. A. McQuarrie, *Statistical Mechanics,* University Science Books, Sausalito, California, 2000

[21] M. P. Allen, D. J. Tildesley, *Computer Simulations of Liquids*, Oxford University Press, New York, 1987

[22] R. Kubo, *J. Phys. Soc. Japan*, 1957, **12**, 570

[23] T. Darden, D. York, L. Pedersen, *J. Chem. Phys*., 1993, **98**, 10089

[24] U. Essmann et al., *J. Chem. Phys*., 1995, **103**, 8577

[25] L. Greengard, V. Rokhlin, *J. Comp. Phys.,* 1987, **73,** 325

[26] D. van der Spoel et al., Gromacs User Manual version 4.0, 2005

[27] U. Stocker, D. Juchli, W. F. van Gunsteren, *Mol. Sim.,* 2003, **29**, 123

[28] J. P. Ryckaert, G. Ciccotti, H. J. C. Berendsen, *J. Comp. Phys.,* 1977, **23**, 327

[29] B. Hess et al., *J. Comp. Chem.,* 1997, **18**, 1463

[30] S. Miyamoto, P.A. Kollman, *J. Comp. Chem.,* 1992, **13**, 952

[31] M. H. Levitt, *Spin Dynamics: Basics of Nuclear Magnetic Resonance,* 2001, John Wiley & Sons, Chichester, England

[32] http://www3.fed.cuhk.edu.hk/chemistry/atomic_mass.html

[33] J. Cavanagh et al., *Protein NMR spectroscopy: principles and practice,* Academic Press, San Diego, California, 1996

[34] R. K. Harris, *Nuclear magnetic resonance spectroscopy: a physicochemical view*, Longman Scientific & Technical, Burnt Mill, England, 1987

[35] F. Bloch, *Phys. Rev*., 1946, **70**, 460

[36] F. Bloch, *Phys. Rev.,* 1956, **102**, 104

[37] R. K. Wangsness, F. Bloch, *Phys. Rev.,* 1953, **89**, 728

[38] A. G. Redfield, *IBM J. Research Develop*., 1957, **1**, 19

[39] C. P. Slichter, *Principles of Magnetic Resonance*, Springer-Verlag, New York, 1978

[40] S. N. Timasheff, G. Xie, *Biophys. Chem.,* 2003, **105**, 421

[41] D. Shortle, FASEB J., 1996, **10**, 27

[42] K. Sasahara, M. Sakurai, K. Nitta, *J. Mol. Biol.,* 1999, **291**, 693

[43] Maurice R. Eftink, *Biophys. J.,* 1994, **66**, 482

[44] Y. Chen, M. D. Barkley, *Biochemistry* 1998, **37**, 9976

[45] C. N. Pace, K. L. Shaw, *Proteins:Suppl*., 2000, **4**, 1

[46] J. K. Myers, C. N. Pace, J. M. Scholtz, *Protein Sci.,* 1995, **4**, 2138

[47] C. Liu et al., *Biochemistry,* 2001**, 40**, 3817

[48] C. M. Johnson, A. R. Fersht, *Biochemistry,* 1995, **34**, 6795

[49] K. C. Aune, C. Tanford, *Biochemistry,* 1969, **8**, 4586

[50] G. I. Makhatadze, *J. Phys. Chem. B,* 1999, **103**, 4781

[51] O. D. Monera, C. M. Kay, R. S. Hodges, *Protein Sci.,* 1994, **3**, 1984

[52] J. A. Schellman, *Biopolymers*, 2004, **34**, 1015

[53] Edward P. O'Brien et al., *Proc. Natl. Acad. Sci.,* 2008, **105**, 13403

[54] H. J. Wong et al., *J. Mol. Biol.,* 2004, **344**, 1089

[55] B. M. P. Huyghues-Despointes, J. M. Scholtz, C. N. Pace, *Nature Struct. Biol.,* 1999, 6, 910

[56] J. Ramprakash et al., *Anal. Biochem*., 2008, **374**, 221

[57] R. L. Baldwin, *Proc. Natl. Acad. Sci. USA*, 1986, **83**, 8069

[58] C. N. Pace et al., *FASEB J.,* 1996, **10**, 75

[59] Y. Nozaki, C. Tanford, *J. Biol. Chem*., 1963, **238**, 4074

[60] D. B. Wetlaufer et al., *J. Am. Chem. Soc.,* 1963, **86**, 508

[61] A. Wallqvist, D. G. Covell, D. Thirumalai , *J. Am. Chem. Soc.,* 1998, **120**, 427

[62] M. Ikeguchi, S. Nakamura, K. Shimizu, *J. Am. Chem. Soc.*, 2001, **123**, 677

[63] S. Shimizu, H. Sun Chan, *PROTEINS*, 2002, **49**, 560

[64] G. Graziano, *J. Phys. Chem. B*, 2001, **105**, 2632

[65] G. Graziano, *Can. J. Chem*., 2002, **80**, 388

[66] S. Chatterjee, I. Basumallick, *J. Chinese Chem. Soc.,* 2007, **54**, 667

[67] D. R. Robinson, W. P. Jencks, *J. Am. Chem. Soc.*, 1965, **87**, 2462

[68] Q. Zou, S. M. Habermann-Rottinghaus, K. P. Murphy, *PROTEINS: Structure, Function and Genetics,* 1998, **31,** 107

[69] G. C. Kresheck, L. Benjamin, J. Phys. Chem., 1964, **68**, 2476

[70] N. F. A. Van der Vegt et al., J. Phys. Chem. B, 2006, **110**, 12852

[71] G. I. Makhatadze, P. L. Privalov, *J. Mol. Biol.*, 1992, **226**, 491

[72] M. I. Paz Andrade, M. N. Jones, H. A. Skinner, *Eur. J. Biochem*., 1976, **66**, 127

[73] C. Tanford, *J. Am. Chem. Soc.,* 1964, **86**, 2050

[74] J. Schellman, *Cmpt. Rend. Trav. Lab. Carlsberg Ser. Chim.,* 1955, **29,** 230

[75] G. C. Kresheck, H. A. Scheraga, *J. Phys. Chem.,* 1965, **69**, 1704

[76] R. H. Stokes, *Aus. J. Chem*., 1967, **20**, 2087

[77] J. Grdadolnik, Y. Maréchal, *J. Mol. Struct*., 2002, **615**, 177

[78] E. G. Finer, F. Franks, M. J. Tait, *J. Am. Chem. Soc.*, 1972, **94**, 4424

[79] X. Hoccart, G. Turrell, *J. Chem. Phys*., 1993, **99**, 8498

[80] H. S. Frank, F. Franks, *J. Chem. Phys*., 1968, **48**, 4746

[81] Y. Khurgin, E. Maksareva, *Fed. Eur. Biochem. Soc.,* 1993, **315**, 149

[82] A. Idrissi, *Spectrochim. Acta A*, 2005, **61**, 1

[83] M. C. Stumpe, H. Grubmüller, *J. Phys. Chem. B*, 2007, **111**, 6220

[84] H. Wei, Y. Fan, Y. Q. Gao, *J. Phys. Chem. B*, 2010, **114**, 557

[85] A. Idrissi, F. Sokolić, A. Perera, *J. Chem. Phys.*, 2000, **112**, 9479

[86] B. Kallies, *Phys. Chem. Chem. Phys.,* 2002, **4**, 86

[87] M.-E. Lee, N. F. A. van der Vegt, *J. Am. Chem. Soc.*, 2006, **128**, 4948

[88] T. Yamazaki et al., *J. Phys. Chem. B*, 2010, **114**, 613

[89] Z. Zhang, Y. Zhu, Y. Shi, *Biophys. Chem.*, 2001, **89**, 145

[90] D. Tobi, R. Elber, D. Thirumalai, *Biopolymers*, 2003, **68**, 359

[91] E. P. O´Brien et al., *J. Am. Chem. Soc.,* 2007, **129**, 7346

[92] R. Zangi, R. Zhou, B. J. Berne, *J. Am. Chem. Soc.,* 2009, **131**, 1535

[93] M. C. Stumpe, H. Grubmüller, *J. Am. Chem. Soc.*, 2007, **129**, 16126

[94] D. K. Klimov, J. E. Straub, D. Thirumalai, *Proc. Natl. Acad. Sci. USA*, 2004, **101**, 14760

[95] R. D. Mountain, D. Thirumalai, *J. Am. Chem. Soc.,* 2003, **125**, 1950

[96] B. J. Bennion, V. Daggett, *Proc. Natl. Acad. Sci. USA*, 2003, **100**, 5142

[97] A. Das, C. Mukhopadhyay, *J. Phys. Chem. B*, 2008, **112**, 7903

[98] A. Caballero-Herrera et al., *Biophys. J.,* 2005, **89**, 842

[99] J. Tirado-Rives, M. Orozco, W. L. Jorgensen, *Biochemistry*, 1997, **36**, 7313

[100] C. A. Schiffer et al., *Biochemistry*, 1995, **34**, 15057

[101] A. Caflisch, M. Karplus, *Structure*, 1999, **7**, 477

[102] L. J. Smith, R. M. Jones, W. F. Gunsteren, PROTEINS, 2005, **58**, 439

[103] C. Camilloni et al., *Biophys. J.*, 2008, **94**, 4654

[104] A. Guerini Rocco et al., *Biophys. J.,* 2008, **94**, 2241

[105] L. Hua et al., *Proc. Natl. Acad. Sci. USA*, 2008, **105**, 16928

[106] M. C. Stumpe, H. Grubmüller, *Biophys. J.*, 2009, **96**, 3744

[107] M. C. Stumpe, H. Grubmüller, *PloS Comp. Biol.*, 2008, **4**, e1000221

[108] A. Das, C. Mukhopadhyay, *J. Phys. Chem. B*, 2009, **113**, 12816

[109] E. Liepinsh, G. Otting, *J. Am. Chem. Soc.,* 1994, **116**, 9670

[110] A. Möglich, F. Krieger, T. Kiefhaber, *J. Mol. Biol.,* 2005, **345**, 153

[111] J. A. Schellman, *Biophys. J.,* 2003, **85**, 108